

# Master Thesis

Dynamic modelling of solar-based power system for off-grid horticulture projects.

## Keshav Krishna





# Master Thesis

## Dynamic modelling of solar-based power system for off-grid horticulture projects.

by

Keshav Krishna

to obtain the degree of Master of Science

at the Delft University of Technology,

to be defended publicly on Monday September 23, 2019 at 10:00 AM.

Student number: 4744241  
Project duration: January 1, 2019 – September 15, 2019  
Thesis committee: Prof. dr. ir. A. Smets, Chair, TU Delft  
Dr. A. Desideri, Daily Supervisor, SOLHO B.V  
Dr. G. Pandraud, Reviewer, TU Delft  
Dr. T. Batista Soeiro External Reviewer, TU Delft

*This thesis is confidential and cannot be made public until December 31, 2021.*

An electronic version of this thesis is available at  
<http://repository.tudelft.nl/>.



# Abstract

With the rise of population, the world energy demands are increasing. This implies a greater pressure on the horticulture industry to increase its production, thus requiring a high energy intensive setup. Thus, sustainable energy sources will play a crucial part in the transition towards sustainability and reducing the carbon emissions in the horticulture sector.

The *Solar PoweRed Horticulture Unit* (SPRHOUT) is the first product of **SOLHO** to cover the energy requirements of horticultural projects completely off the grid. In this thesis, the original results related to the steady-state and dynamic modelling of the Solar Powered Horticultural Off-Grid Unit (SPRHOUT) developed by SOLHO are outlined.

A techno-economic case study is performed for a location in Greece, where SPRHOUT system is compared with a system consisting of PV + gas burner. The preliminary analysis shows that the CAPEX and OPEX of SPRHOUT for a 5 Ha greenhouse is lower as compared to PV + gas burner system mostly due to the cost of batteries.

The second part of the result involved developing a dynamic model based on the object-oriented programming language, Modelica. The control strategy for the model was analysed for a test case of  $1 \text{ kW}_{el}$  electric load for a location in Jeddah, Saudi Arabia with the simulations showing satisfactory performance of the SPRHOUT system. An economic analysis based on net present value and payback time was also performed for a scaled up facility having an electrical load of 50 kW. The results compared the NPV with respect to the electric grid prices and an optimum value for the solar field sizing was found for which the NPV was highest. A parametric analysis was also performed for the NPV versus the gas prices which displayed a need for subsidies in the form of carbon tax for which the project is competitive with the current gas prices.



# Acknowledgements

Finally, the thesis is coming to an end. I would like to thank Dr. Arno Smets for agreeing to be my supervisor. His input was extremely valuable and he gave me the independence to work at my own pace which helped me a lot. Part of the reason I came to TU Delft was because I saw Arno's lectures on EdX. Having him as my supervisor was amazing.

I have to thank Adriano Desideri for giving me the opportunity to work at an exciting project in a dynamic company. Working on a new software based platform is not easy and his patience never seemed to wane. He always motivated to ask questions and that was extremely helpful. I learned a lot and have nothing but gratitude for that. I am also grateful to Simone for his guidance as well. To Adriano, we still have the final match of ping-pong left. I hope it is as intense as this thesis was.

I guess I have to thank TU Delft as well since I did learn a lot from this university. I am now qualified to give out some life lessons as well. I will write a book about it someday. Please buy it. I also met some wonderful people in this journey who carried me through this thesis like a breeze. Its always great to have people by your side who are ready to help you out when in need.

Finally, I would like to thank my parents for their support. Also they didn't ask a lot of questions and supported me, unlike other Indian parents who would probably be freaking out about why it took me so long to finish this thesis. Yup I am eternally happy I didn't have to go through that.

I am also happy that during this period of my thesis, Liverpool F.C. won the Champions League. Sorry Ajax!

Lastly, a great person once said, "*Life is 1% inspiration, 98% perspiration and 2% attention to detail*"

*Keshav Krishna*

*TU Delft*



# Contents

<b>Abstract</b>	<b>iii</b>
<b>Acknowledgements</b>	<b>v</b>
<b>List of Figures</b>	<b>ix</b>
<b>List of Tables</b>	<b>xiii</b>
<b>1 Introduction</b>	<b>1</b>
1.1 Energy Scenario . . . . .	1
1.2 Current Technologies . . . . .	4
1.3 Outline of the thesis and research questions . . . . .	6
<b>2 SPRHOUT</b>	<b>7</b>
2.1 Brief description of SPRHOUT . . . . .	7
2.2 State of the art solutions and competitive analysis . . . . .	9
2.2.1 SPRHOUT sizing specifications. . . . .	13
2.2.2 PV system sizing specification . . . . .	14
2.2.3 CAPEX comparison . . . . .	16
<b>3 Dynamic Model Description</b>	<b>19</b>
3.1 Dynamic Modelling and Modelica . . . . .	19
3.2 Solvers used for model simulation . . . . .	20
3.2.1 DASSL Solver . . . . .	20
3.3 ThermoCycle Library Description. . . . .	20
3.3.1 Cell1DimInc . . . . .	22
3.3.2 Flow1DimInc . . . . .	22
<b>4 SPRHOUT Modelica Model</b>	<b>25</b>
4.1 SPRHOUT Library . . . . .	25
4.2 SPRHOUT component description. . . . .	26
4.2.1 Flat plate solar collector. . . . .	26
4.2.2 Thermal Energy Storage (TES) . . . . .	29
4.2.3 Power Block . . . . .	31
4.2.4 Control Unit. . . . .	32
4.2.5 Gas Burner . . . . .	32
4.2.6 Expansion Tank . . . . .	34
4.2.7 Fan . . . . .	35
4.3 SPRHOUT Overview . . . . .	36
<b>5 Control Strategies</b>	<b>37</b>
5.1 Initial Control Strategy. . . . .	37
5.2 Final Control strategy . . . . .	39

---

<b>6</b>	<b>Simulation Results and Discussion</b>	<b>41</b>
6.1	Model Inputs and parameters . . . . .	41
6.1.1	Control logic analysis . . . . .	41
6.1.2	Economic analysis . . . . .	43
6.2	SPRHOUT control logic analysis . . . . .	45
6.3	SPRHOUT economic analysis . . . . .	54
<b>7</b>	<b>Conclusions</b>	<b>59</b>
7.1	Recommendations for future work . . . . .	61
	<b>Bibliography</b>	<b>63</b>

# List of Figures

1.1	Probabilistic projections of the total population of the world[1]. It can be seen that the population will cross the 10 billion mark by 2050, which is alarming. . . . .	1
1.2	World energy consumption projection by energy source. It can be seen that the dependence on coal and petroleum still is significantly higher than the renewables. . . . .	2
1.3	Increase in use of sustainable energy in the Netherlands between the year 2010 and 2015. . . . .	3
2.1	Schematic Diagram of energy production using Solar thermal energy and storage. . . . .	7
2.2	T-S diagram for an organic rankine cycle for R-123 fluid. Process 3-4 shows the evaporation process. The fluid is then sent to the turbine for generation of electricity, which can be seen from point 4-5. Finally the fluid is condensed from 5-1 and the process repeats. . . . .	8
2.3	Illustrative diagram showing the SPRHOUT system and the greenhouse.	9
2.4	Load Data required by a greenhouse facility in Greece. (a) shows the electrical load in kW for the plant for summer i.e. months of June, July and August. (b) shows the electrical load in kW for the plant at that location for winter i.e months of December, January and February. . . .	11
2.5	Load Data required by a greenhouse facility in Greece. (a) shows the thermal load in kW for the plant for summer i.e. months of June, July and August. (b) shows the thermal load in kW for the plant at that location for winter i.e months of December, January and February. . . . .	12
2.6	Block diagram for the SPRHOUT system. $P_{ELECTRICAL}$ and $P_{THERMAL}$ represents the electrical and thermal power input to the greenhouse. . .	13
2.7	Block diagram for the PV + gas burner system. $P_{ELECTRICAL}$ and $P_{THERMAL}$ represents the electrical and thermal power input to the greenhouse. . .	15
3.1	Schematic representation of the structure of ThermoCycle modelica library. . . . .	21
3.2	Schematic representation of Cell1DimInc model in Dymola graphical user interface(GUI). . . . .	22
3.3	Schematic representation of Flow1DimInc model in Dymola graphical user interface(GUI). . . . .	23
4.1	Schematic representation of the structure of SPRHOUT modelica library.	26
4.2	Diagram of flat plate solar collector model from Dymola graphical user interface (GUI). The model is composed of AbsFlatPlate model connected with the Flow1Dim model. . . . .	27
4.3	Schematic representation of TES block in Dymola. . . . .	29

4.4	Representation of the Power Block model from the Dymola graphical user interface (GUI). . . . .	31
4.5	Block representation of the PI controller model used in Dymola. . . . .	32
4.6	Representation of the gas burner model from the Dymola graphical user interface (GUI). . . . .	33
4.7	Representation of the Expansion tank model from the Dymola graphical user interface (GUI). . . . .	34
4.8	Representation of the SPRHOUT model used for simulation in Dymola.	36
5.1	The initial control flow chart. The initial check is for the load represented by $Load_{EL}$ . . . . .	38
5.2	The final control flow chart. The initial check is for the load represented by $Load_{EL}$ . . . . .	40
6.1	Load demanded by the greenhouse for the whole year for the location in Jeddah, Saudi Arabia. The red dashed line represents the thermal load [W] and the blue line represents the electric load [W] of the greenhouse.	45
6.2	Dynamic simulation results of the SPRHOUT model during a reference winter day in Jeddah, Saudi Arabia. Temperature sensors TT001 and TT002 represents the normalised inlet and outlet temperatures of the solar field. $m_{SF}$ represents the mass flow through the solar field and the red line represents the Irradiation. . . . .	47
6.3	Dynamic simulation results of the SPRHOUT model during a reference winter day in Jeddah, Saudi Arabia. The left y axis represents the energy in TES given in MJ. The right y-axis represents the thermal and electrical loads in W. . . . .	47
6.4	Dynamic simulation results of the SPRHOUT model during a reference summer day in Jeddah, Saudi Arabia. Temperature sensors TT001 and TT002 represents the normalised inlet and outlet temperatures of the solar field. $m_{SF}$ represents the mass flow through the solar field. On the right y-axis, the irradiation incident on the solar field is plotted. . . .	49
6.5	Dynamic simulation results of the SPRHOUT model during a reference summer day in Jeddah, Saudi Arabia. The left y axis represents the energy in TES given in MJ. The right y-axis represents the thermal and electrical loads in W. . . . .	49
6.6	Dynamic simulation results of the SPRHOUT model during a reference spring day in Jeddah, Saudi Arabia. Temperature sensors TT001 and TT002 represents the normalised inlet and outlet temperatures of the solar field. $m_{SF}$ represents the mass flow through the solar field. On the right y-axis, the irradiation incident on the solar field is plotted. . . .	51
6.7	: Dynamic simulation results of the SPRHOUT model during a reference spring day in Jeddah, Saudi Arabia. The left y axis represents the energy in TES given in MJ. The right y-axis represents the thermal and electrical loads in W. . . . .	51

6.8	Dynamic simulation results of the SPRHOUT model during a reference autumn day in Jeddah, Saudi Arabia. Temperature sensors TT001 and TT002 represents the normalised inlet and outlet temperatures of the solar field. $m_{SF}$ represents the mass flow through the solar field. On the right y-axis, the irradiation incident on the solar field is plotted. . . . .	53
6.9	Dynamic simulation results of the SPRHOUT model during a reference autumn day in Jeddah, Saudi Arabia. The left y axis represents the energy in TES given in MJ. The right y-axis represents the thermal and electrical loads in W. . . . .	53
6.10	Energy cash flow analysis. The figure shows the NPV vs the electricity price for different sizing of the solar field using the solar multiple factor. Figure represents SM=1.5,2,3 for which the NPV is calculated. . . . .	54
6.11	Optimum sizing of the solar field based on NPV. The configuration of SM=2 results in maximum NPV for the project in Jeddah, Saudi Arabia, thus representing the optimum sizing for the solar field. . . . .	56
6.12	Energy cash flow analysis. The figure shows the NPV vs the gas price for different sizing of the solar field using the solar multiple factor. Figure represents SM=1.5,2,3 for which the NPV is calculated. . . . .	57
6.13	Energy cash flow analysis but with carbon tax implemented. The figure shows the NPV vs the gas price for different sizing of the solar field using the solar multiple factor. Figure represents SM=1.5,2,3 for which the NPV is calculated. . . . .	58



# List of Tables

2.1	Technical specifications of SPRHOUT system for location in Greece. . .	14
2.2	Technical specifications for a PV and gas burner system for location in Greece. . . . .	15
2.3	Capital expenditure of the SPRHOUT system. . . . .	16
2.4	Operating expenditure of different components in SPRHOUT system. .	16
2.5	Operating expenditure of different components in PV+gas burner system. . . . .	16
2.6	Capital expenditure of PV + gas burner system. . . . .	17
6.1	Solar field model parameters. . . . .	42
6.2	TES simulation parameters . . . . .	42
6.3	PI control parameters . . . . .	43
6.4	Expansion tank parameters . . . . .	43
6.5	Economic Parameters for a SPRHOUT plant in Jeddah, Saudi Arabia. CAPEX represents the capital expenditure and the OPEX represents the operating expenditure of the whole plant including SPRHOUT and greenhouse. . . . .	55



# Introduction

## 1.1. Energy Scenario

A major step towards climate change was taken, when around 195 countries of the world signed the Paris Agreement in 2016. The main objective as stated in the Paris Agreement is to reduce the global temperature rise this century to well below 2 degree Celsius. Furthermore, efforts are being made to limit the increase in temperatures even more to 1.5 degree Celsius [2].

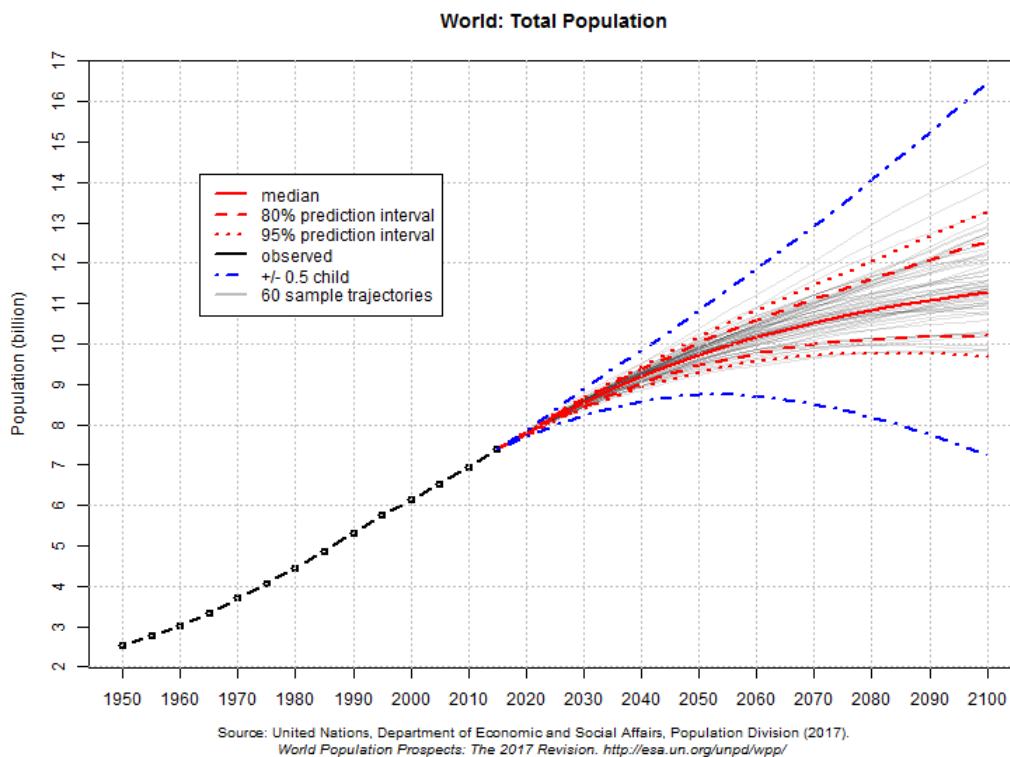


**Figure 1.1:** Probabilistic projections of the total population of the world[1]. It can be seen that the population will cross the 10 billion mark by 2050, which is alarming.

With the rise of population, the world energy demands will increase. The United States Energy Information Administration projects that the non-OECD countries will account for approximately 64% of the global energy consumption by 2040 [3]. The dependence on fuels such as natural gas and petroleum increases by 2040 along with an increase in renewables. From figure 1.2, it can be safely stated that fossil fuels are still major contributors to the energy production due to their availability and cost.

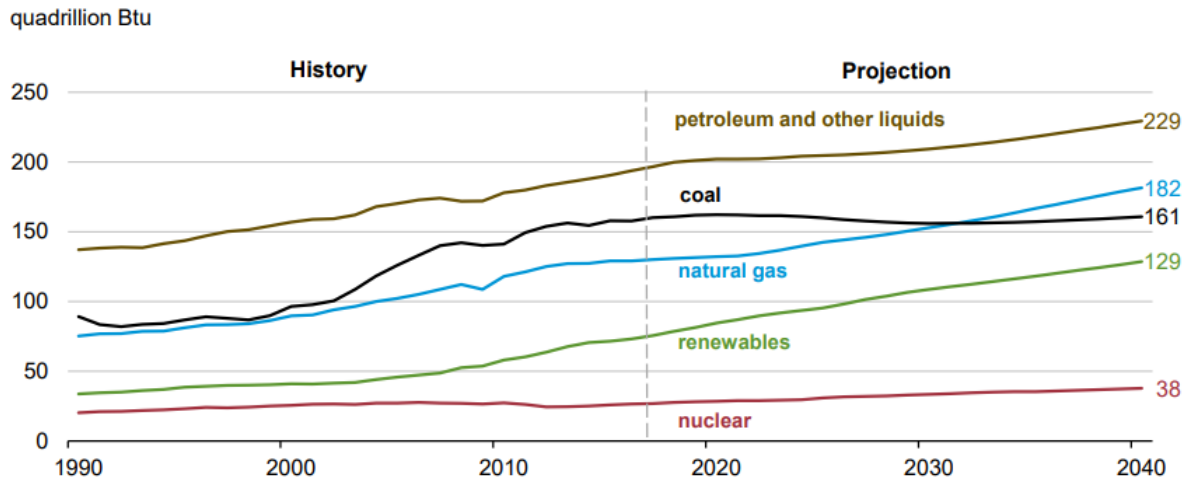


**Figure 1.2:** World energy consumption projection by energy source. It can be seen that the dependence on coal and petroleum still is significantly higher than the renewables.

According to various studies, the effects of global warming will not just impact certain regions but will have an overall effect on the world. Various industries are being affected by global warming and agriculture industry is one of them. It has been projected by the United Nations that the world population will be approximately 10 billion by the year 2050 as shown by figure 1.1. Thirty years from now, there will be 2 Billion more people living on earth, almost 90% of them will be concentrated in the so-called sun belt region [4]. Agriculture is largely dependent on climate and changes in the temperature and carbon dioxide levels can disrupt the natural ecosystem [5]. Due to these changes, the food availability will be disrupted causing a reduced access to food and tarnish the food quality. Agriculture will have to double food production to sustain the global population growth, with fewer resources and reduced environmental impact.

A part of the agriculture industry is the horticulture industry which consists of production of fruits and vegetables. Netherlands is the third largest exporter of fruits and vegetables in the world, only behind Spain and Mexico [6]. The horticulture industry in Netherlands plays an important role in export fruits and vegetables on a large scale. This also implies that the energy demands of the horticulture industry is quite high. The energy consumption in greenhouses is mainly based on heating and electricity (lighting) which are provided using gas and the national electricity grid. Looking at the horticulture industry in the Netherlands, the Dutch government set an objective of reducing the CO<sub>2</sub> emissions from 8.1 Mton in 2010 to 6.2 Mton by 2020 [7]. It can also be observed that there was a decline in energy consumption per m<sup>2</sup> of the cultivation area implying a transition to energy efficient technology for heating and electricity. The use of sustainable energy sources has also increased from 2010. From 2010-2015,

the share of renewable energy usage increased by 110 % . In terms of numerical figures, there was an increase from 2.4 PJ in 2010 to 5.0 PJ by 2015 as shown in figure 1.3. During this time, the area covered by greenhouses also declined from 10,307 hectares to 9,206 hectares but it should be noted that this declined occurred due to the economic situation [7].

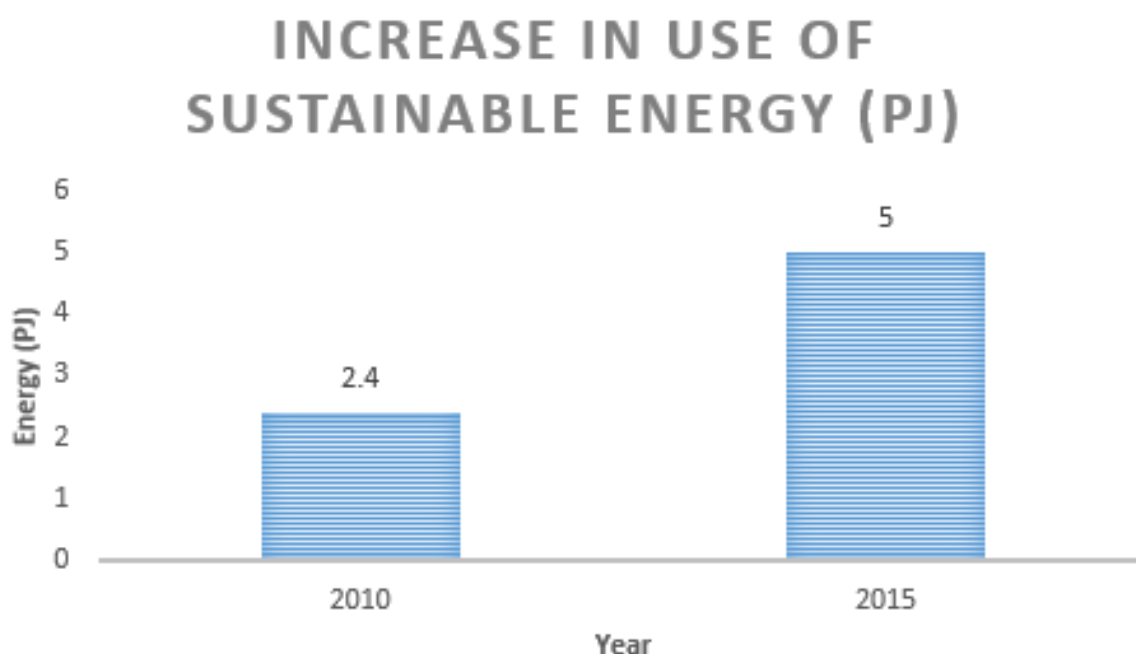


**Figure 1.3:** Increase in use of sustainable energy in the Netherlands between the year 2010 and 2015.

Technology will play a crucial part in the transition towards sustainability and reducing the carbon emissions in the horticulture sector and therefore has to be integrated into the horticulture practices in order to utilise its potential. The Netherlands is one of the leading countries in integrating technology to maximise its horticulture potential. Over the years, the total area of greenhouses has increased by 17% [8]. Most of the greenhouses are now reusing organic waste and utilising rainwater for irrigation. Due to horticulture being an energy intensive industry, the Dutch government also laid out policies to increase the contribution of sustainable energy to around 4% of the total energy input [9]. It is clear that as the population increases, the contribution of renewable energy in the energy intensive horticulture practices has to increase, not just in Netherlands, but all over the world.

Thus, there is a need to integrate renewable energy technologies into horticulture facilities in order to better manage the resource and maximise the output without relying on traditional fossil-based energy sources. The Food and Agricultural Organisation of the United Nations (FAO) has defined the “Save and Grow” paradigm to minimise the horticulture’s impact on climate change adopting “sustainable intensification of greenhouse”[10]. Public and private activities to integrate renewable energy technologies (RES) to horticultural facilities have recently increased. Sundrop farms in Australia have developed an integrated system which utilises solar energy to pro-

duce fresh water for irrigation and electricity to power a 20 Ha greenhouse facility [11]. Another example is the use of geothermal energy to provide the energy needs of greenhouses in Northern Europe, especially in countries such as Switzerland and Sweden [12].

## 1.2. Current Technologies

Most of the manufacturers of greenhouses are opting to switch to renewable energy sources to power the energy needs of the greenhouses. As mentioned in section 1.1 countries such as Switzerland, Sweden and Australia are adopting such methods. De centralised research and development of decentralised renewable energy-based systems can play a role in the process of decarbonizing horticulture.

One of the main energy consumptions in a greenhouse is heating. Countries such as Iceland have major heating requirements due to its cold climate. A study performed for average energy consumption for heating for a group of greenhouses in Iceland showed that for a greenhouse without artificial lighting, the average energy consumption was 5.76 GJ/m<sup>2</sup>/yr [13]. Geothermal energy provides 87% of all the heating and hot water requirements of buildings in Iceland and is used as a primary source of heating by greenhouses.

There are similar plans by Netherlands government to replace natural gas by geothermal energy to provide heating for the greenhouses. The Netherlands aims to reduce its CO<sub>2</sub> equivalent emissions by 40% by 2030 compared to 2015[14]. Around 40% of the dutch emissions are due to heat consumption. By switching to geothermal energy, it plans to reduce 0.3 megatons per year of CO<sub>2</sub> because of geothermal energy [15]. This switch to geothermal energy has its own problems associated with it. Due to the drilling in the north of the Netherlands, there is a high risk of earthquakes, which might make geothermal energy unsuitable for some places in the Netherlands.

Other renewable energy technologies are also being investigated. One of the technologies in focus is solar energy. A recent collaboration by the Dutch government with some of the leading Dutch companies plans to use both solar PV and solar thermal energy technologies to provide electricity and heating in countries such as Kenya and Ethiopia in Africa which are characterised by an average of 4-6 kWh/m<sup>2</sup>/yr of solar energy [16]. Under this collaboration, a solar powered greenhouse was put in practice in a test farm in Naivasha in Kenya where a combination of solar PV and solar thermal technologies aimed to reduce the energy costs by 40% [17].

Another such example can be seen where Rebound Technologies have used solar thermal technology to provide energy for a cold storage in Mozambique in Africa. The technology, aptly named SunChill, is an off-grid refrigeration setup that transforms solar thermal energy into refrigeration using solid refrigerants. [18].

For large scale greenhouses (1 to 20 hectares), SOLHO B.V. has started investigating since 2017, the commercial potential of a solar thermal based energy system. The unit is called SPRHOUT (Solar PowerRed Horticultural Off-grid UniT) and it integrates a solar field of thermal collectors together with a thermal energy storage and a power

unit, based on the Organic Rankine Cycle (ORC) concept.

Various scientific publications have focused on assessment of the solar based ORC and thermal storage plants. The publication by Casati et al. [19] simulates a 100 kWe power plant with parabolic trough collectors and thermal energy storage and yields a solar-to-electric design efficiency of 18% . The control strategy for the system relied on keeping the temperature at the outlet of the solar field constant according to the transient conditions.

Using thermal storage is a key part in integrating solar thermal technology to produce electricity. One such example is shown in paper by Bayon [20] which simulates a thermocline storage for a solar thermal power plants. A one dimensional model was developed for simulating thermocline storage tanks with different mediums. The behaviour of the tank was described by dimensionless variables in the thermal equation, which resulted in the design equations for maximum theoretical efficiency to be established. According to Bayon, the storage capacity and charging/discharging time is dependent of the power required.

Another scientific publication [21] focuses on the dynamic modelling of a low capacity Organic Rankine Cycle (**ORC**) system. Since an ORC unit can be described as a set of differential algebraic equations, a robust solver is used to simulate the dynamic system. The object oriented programming language Modelica was used as it simulates complex physical processes with ease. The paper describes the dynamic model using the ThermoCycle library where different components such as pumps, heat exchangers, tank and pressure drop valves are modelled individually. This model is validated using a 11 kWe ORC test rig. The steady state validation shows the simulation result and experimental data for net output power are comparable with an error of below 5%. This paper shows the scope for growth of ORC technologies.

In the paper by Casati et al [22], a small scale solar Organic Rankine Cycle plant consisting of Thermal Energy Storage (**TES**) is described. A Concentrated Solar Power (**CSP**) technology is used in the form of parabolic trough collectors with evacuated absorber tubes. The TES is modelled to include various thermal fluids such as silicon oils for application purposes. The control strategy developed in the paper focuses on keeping the temperature at the outlet of the solar field at a nominal value under transient conditions. Simulating a 100 kW<sub>e</sub> case study plant, a solar-to-electric efficiency of 18% was calculated under set conditions. The system reaction to cloud coverage was also simulated and resulted in the solar input dropping to 10% of its nominal value. Overall, the paper positively assessed the feasibility of the solar thermal ORC plant.

### 1.3. Outline of the thesis and research questions

As discussed in the previous section, multiple green technologies have been applied to cover the energy requirements of the horticulture facilities. This thesis focuses on the following research questions that arise when developing solar powered technologies for off-grid horticultural projects:

- How does the proposed solar-based energy system, the SPRHOUT, compare to photovoltaic technology?
- How can you improve the control strategy to ensure optimum running of the plant under real operating conditions?

In order to answer the research questions mentioned above, the thesis is divided into 7 main chapters. Chapter 2 gives a brief description about the SPRHOUT system and presents a techno-economic analysis of the SPRHOUT with respect to a photovoltaic (PV) system. In chapter 3, the dynamic model description is explained and the object-oriented programming language Modelica is introduced. Chapter 4 talks about the SPRHOUT Modelica model and the control strategies that are used for the whole model is discussed in chapter 5. The results of the simulations are presented in chapter 6 and based on that the conclusions and scope for future work are exhibited in chapter 7.

# 2

## SPRHOUT

### 2.1. Brief description of SPRHOUT

The *Solar PowerRed Horticulture Unit* (SPRHOUT) is the first product of **SOLHO** to cover the energy requirements of horticultural projects completely off the grid. The SPRHOUT uses the sun to generate all the streams required by a greenhouse facility: electricity, thermal energy at 60-80°C for heating and up to 140°C to run specific subsystems, in case they are needed (like adsorption chillers and sea water desalination units).

The SPRHOUT unit is based on the following technologies:

- A field of solar thermal collectors (SF) converting the sun energy into thermal energy, which can count on different SF technologies (such as concentrating or flat plate collectors) depending on the specific application scenario.
- A power unit (PU) converting thermal energy into electricity, based on the Organic Rankine Cycle (ORC) technology.
- A Thermal Energy Storage (TES) system allowing round the clock operation of the PU and all other units. The TES is based on a modular dual media single tank concept developed by SOLHO and it is called TESMOD.

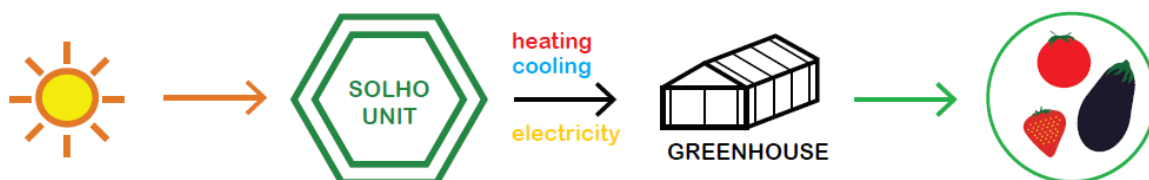


**Figure 2.1:** Schematic Diagram of energy production using Solar thermal energy and storage.

An ORC uses organic fluid whose boiling point occurs at a temperature that is lower than the water-steam phase change. This technology has been widely used for heat

recovery applications as well as converting low temperature heat into electricity. The application of ORCs is popular for waste heat recovery, biomass power plants, solar thermal plants and geothermal plants among others. The working principle for the organic Rankine cycle is the same as that of the Rankine cycle where the working fluid enters the boiler, gets heated up and then moves to an expansion device such as a turbine and finally through a heat exchanger where it is re-condensed. As the fluid used doesn't reach its condensation temperature, it can be reused to preheat the liquid before it enters the evaporator.

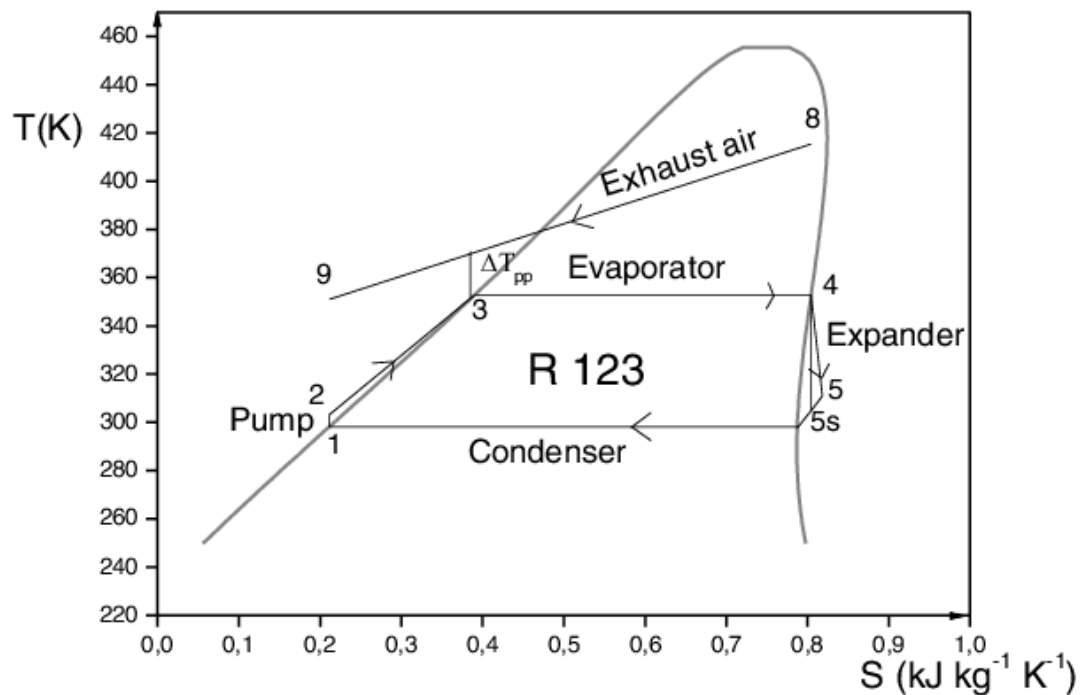


**Figure 2.2:** T-S diagram for an organic rankine cycle for R-123 fluid. Process 3-4 shows the evaporation process. The fluid is then sent to the turbine for generation of electricity, which can be seen from point 4-5. Finally the fluid is condensed from 5-1 and the process repeats.

The operating system can be summarised as follows: depending on the application and location of the plant, the SPRHOUT unit harvests solar energy through a field of flat-plate solar collectors (temperature up to  $140^{\circ}\text{C}$ ). This modular solar technology is well established and commercially available.

The SPRHOUT unit stores the collected solar energy thanks to the modular Thermal Energy Storage (TESMOD) system developed by SOLHO to meet the specific requirements of the greenhouse in terms of temperature levels, sizes (approximately 100 times smaller than grid-connected CSP plants) and reliability (autonomous operation is required).

The stored energy can be withdrawn when needed from the TESMOD to heat up the greenhouse and/or to be converted into electricity by means of an ORC thermal

engine, which is a commercially available technology proven to be preferable over steam turbines in the range of temperatures and sizes of interest. The SPRHOUT unit features a backup unit (e.g., a bio-gas or fossil fuel burner) which makes up for missing solar input (if needed) and guarantees 100% redundancy minimising the risks for the crop.

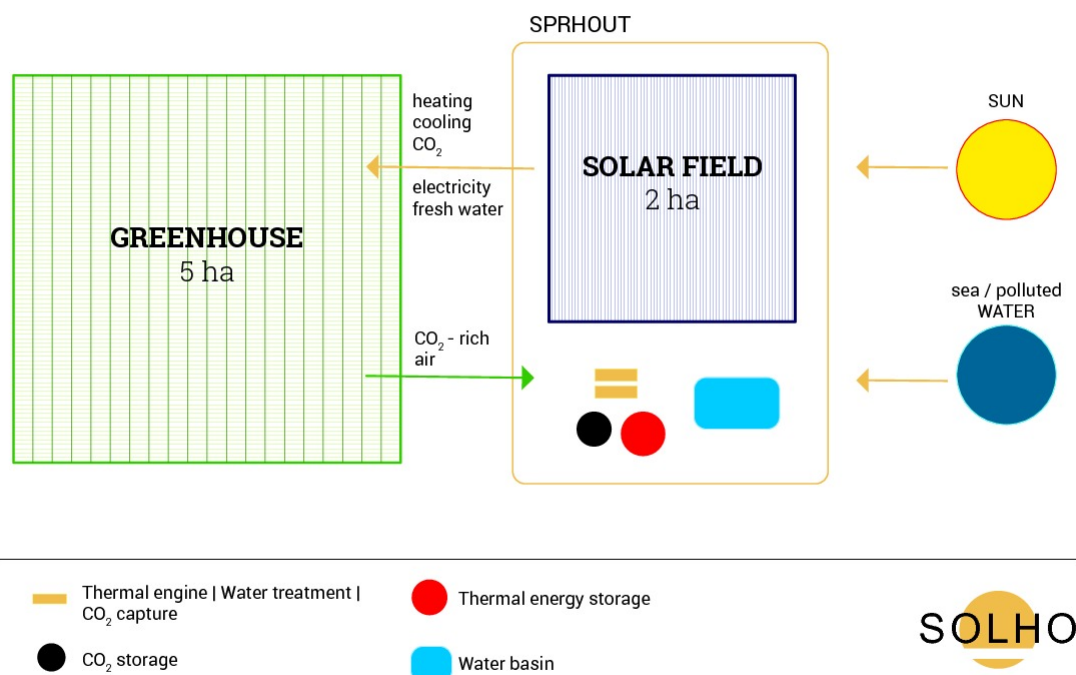


**Figure 2.3:** Illustrative diagram showing the SPRHOUT system and the greenhouse.

## 2.2. State of the art solutions and competitive analysis

To analyse the SOLHO's competitive scenario, we need to first account for the technologies currently used to power greenhouse plants:

- State-of-the-art high-tech greenhouse facilities are connected to an electric grid for lightening, pumping and ventilation purposes, and to a natural gas network to feed the burners generating the required thermal energy. Another solution, mainly adopted in Northern Europe, consists in the adoption of combined heat and power (CHP) units featuring gas engines that co-generate electricity and heat. This approach is profitable when the greenhouse electric consumption is relatively high and under regulatory frameworks which allow to sell excess electricity to the grid. In the absence of a reliable gas network, liquified petroleum gas (LPG) transported with tanker trucks can be used to feed the burners and/or the CHP units. However, the fuel cost and the greenhouse operating costs in general are bound to be much higher in this case - not to mention the environmental

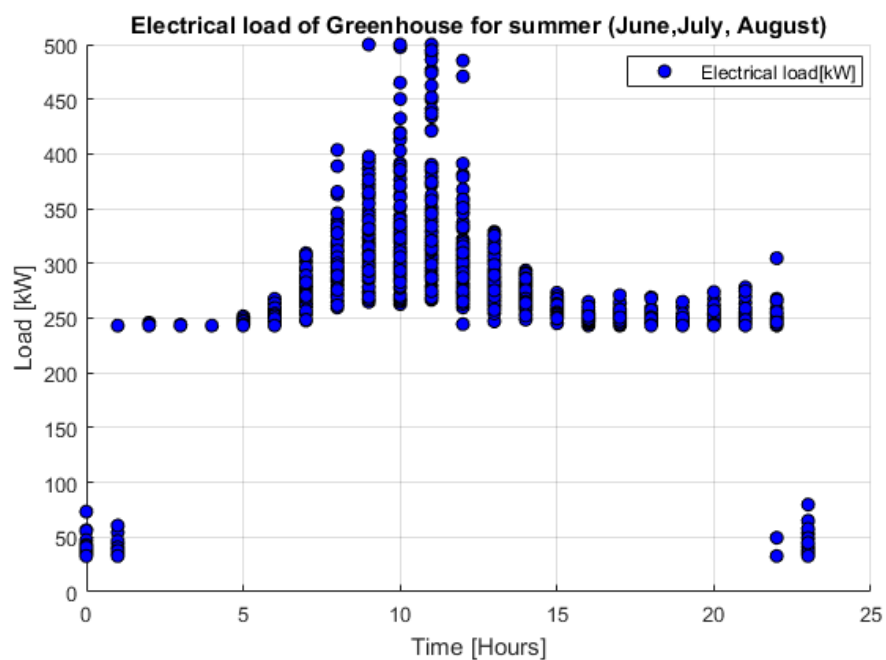
impact.

- The exploitation of renewable energy sources to power greenhouses is increasingly gaining interest. A notable example is represented by the use of geothermal energy: heating and cooling power are withdrawn from the underground and distributed into the greenhouse with very low operational costs and environmental impact. However, the availability of economically exploitable geothermal reservoirs is geographically restricted, and the costs related to the drilling of the well make the solution uneconomical in most regions. Finally, this approach does not allow to generate the electricity needed by the greenhouse. Solutions integrating photovoltaic (PV) panels have been deployed recently, mostly in France and Spain, with the aim of reducing the electricity withdrawn from the grid. PV does not deliver heat, as a consequence additional equipment is required to provide this fundamental input to the greenhouse.

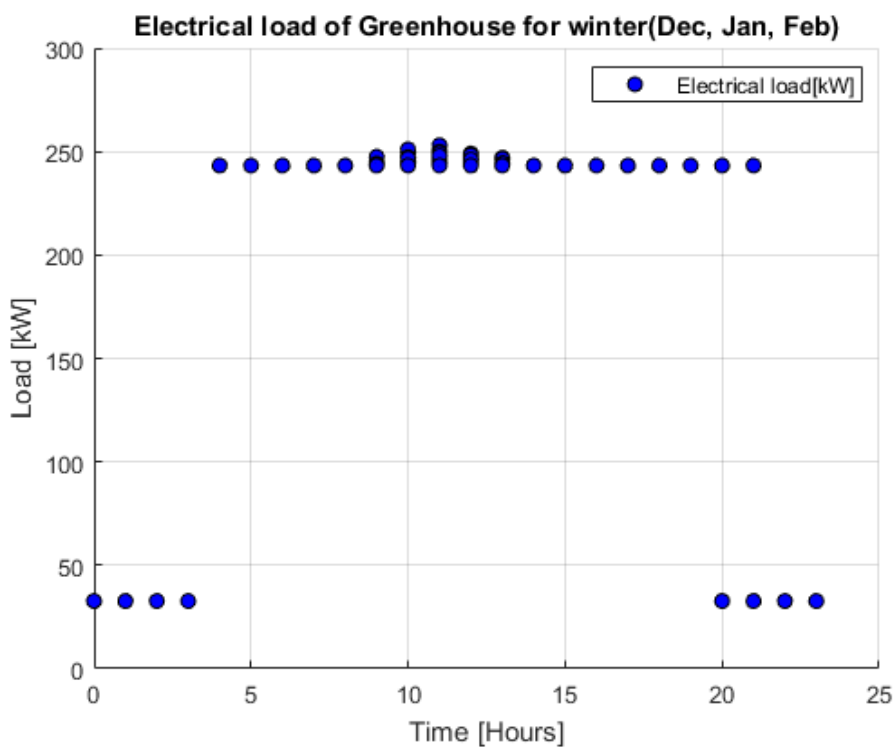
In order to precisely assess the benefits offered by the SPRHOUT, an evaluation of the capital and operating costs of the SPRHOUT and a PV-based solution coupled with a gas burner has been performed and results are reported in this section.

The capital expenditure (CAPEX), is the cost incurred when a company buys, maintains or improves its fixed assets. CAPEX usually increases the value of an asset beyond a given tax year. Similarly, OPEX or operating expenditure, is the cost incurred in running the plant or facility.

For the comparison, a 5-ha greenhouse facility built in Petrousa, Greece is considered. The SPRHOUT and the PV system are designed to cover the electricity and thermal energy requirements of the greenhouse facility.

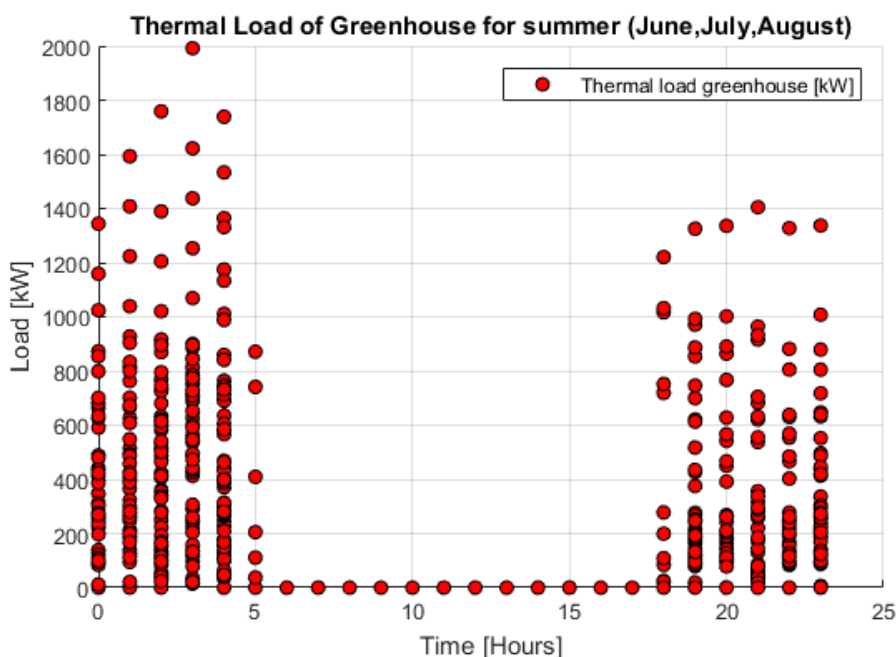


(a)

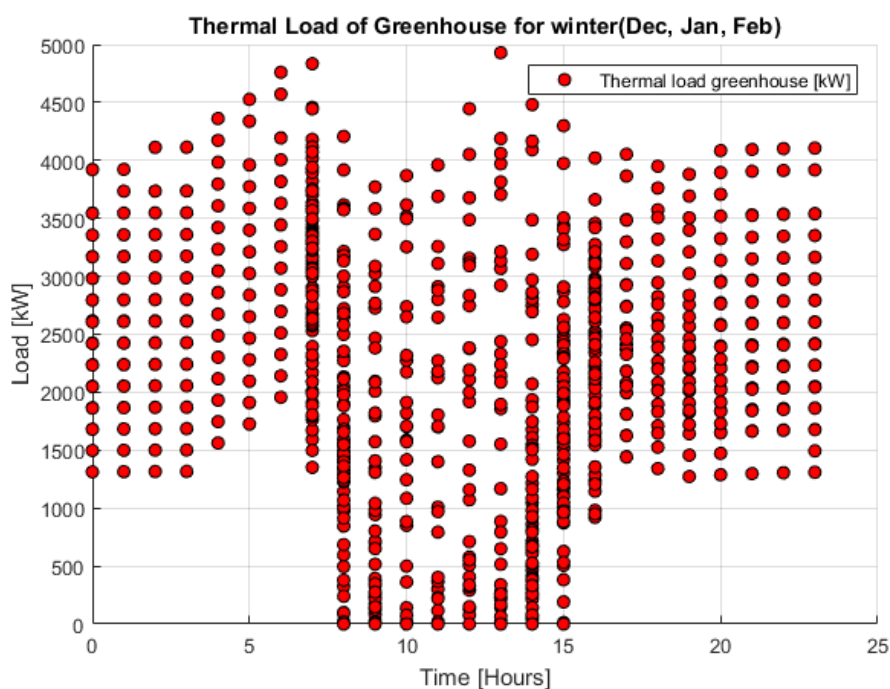


(b)

**Figure 2.4:** Load Data required by a greenhouse facility in Greece. (a) shows the electrical load in kW for the plant for summer i.e. months of June, July and August. (b) shows the electrical load in kW for the plant at that location for winter i.e. months of December, January and February.



(a)



(b)

**Figure 2.5:** Load Data required by a greenhouse facility in Greece. (a) shows the thermal load in kW for the plant for summer i.e. months of June, July and August. (b) shows the thermal load in kW for the plant at that location for winter i.e. months of December, January and February.

As can be seen from the figure 2.4a, the electrical load reaches its peak during the summer when fans are used to keep the indoor temperature within the required threshold and it amounts to  $500 \text{ kW}_{el}$ . As the solar-based energy systems, the SPRHOUT and the PV unit, are considered to operate off-grid, their nominal power is set at 500

$\text{kW}_{el}$ . Similarly, the thermal load reaches its peak during the winter when the heating is required by the greenhouse in order to keep the temperatures inside at a nominal level, as compared to the low ambient temperature. This load amounts to approximately  $5000 \text{ kW}_{th}$ . It is also seen from figure 2.5b that the heat required is higher during the night as compared to day time.

### 2.2.1. SPRHOUT sizing specifications

The SPRHOUT system block diagram is reported in figure 2.6.

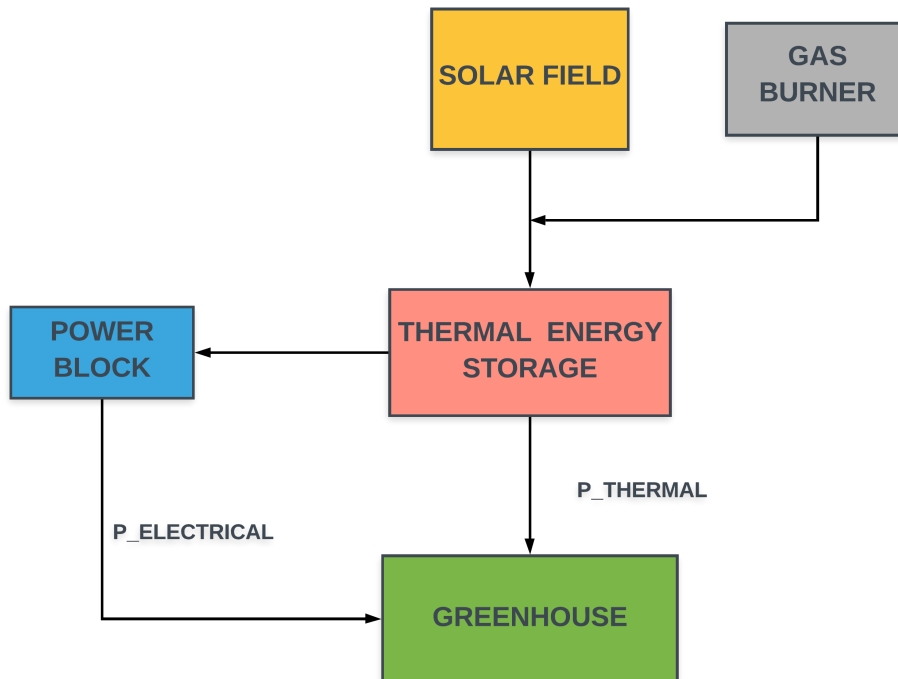


**Figure 2.6:** Block diagram for the SPRHOUT system.  $P_{ELECTRICAL}$  and  $P_{THERMAL}$  represents the electrical and thermal power input to the greenhouse.

Single glass flat plate solar thermal collector is selected for the solar field. At nominal conditions, ( $\text{GHI}: 1000 \text{ W/m}^2$ ,  $T_{amb}: 25^\circ\text{C}$ ) the field is characterised by a solar to thermal efficiency of 63%, heating the heat transfer fluid from  $70$  to  $95^\circ\text{C}$ . The ORC plant nominal power is fixed at  $500 \text{ kW}_{el}$ . The efficiency of the machine is 10% with an evaporator inlet temperature of  $90^\circ\text{C}$ . The area of the solar field is dependent on the nominal electric power required by the ORC and the solar multiple as shown in the expression as follows:

$$Area_{SF} = \frac{P_{Elorc} \cdot SM \cdot 1000}{\eta_{orc} \cdot \eta_{sf} \cdot Irr_{nominal}} \quad (2.1)$$

Where SM is the solar multiple <sup>1</sup>,  $\eta_{ORC}$  is the efficiency of the power unit,  $\eta_{SF}$  is the efficiency of the solar thermal panels and  $Irr_{nominal}$  is the nominal irradiation assumed to be 1000 W/m<sup>2</sup>. Using the expression, the solar field area was calculated to be approximately 16000 m<sup>2</sup>.

In order to cover the energy requirements of the greenhouse off-grid, the TES was sized to provide the thermal energy required to operate the Power unit at its nominal conditions for 10 hours. This led to a total thermal energy stored to be 50000 kWh. The volume and the dimensions of tank were calculated accordingly. Table 2.1, shows the technical specifications for the SPRHOUT system. A gas burner was used as contingency for situations where the irradiation from the solar field is insufficient to provide thermal energy to the TES to match the load requirements of the greenhouse. In such cases, the gas burner operates and provides the energy deficit which helps in running the power unit without any interruptions.

	Parameter		Units
<b>Power Block Specifications</b>	PeI	500	kWeI
	ORC		
	Efficiency_ORC	0.10	
	T_inlet ORC	90	degC
	T_outlet ORC	80	degC
<b>Solar Field Specification</b>	Panel Efficiency	0.63	-
	SF Area (Solar multiple = 2)	15994.37	m2
	SF nominal power	10000	kWth
	SF Tmean	85	degC
<b>TES Specification</b>	Stored Energy	50000	kWh
	Volume of media	4278.14	m3
	Diameter of vessel	23.34	m
	Height of vessel	10	m
	Volumetric energy density	11.69	kWh/m3

**Table 2.1:** Technical specifications of SPRHOUT system for location in Greece.

### 2.2.2. PV system sizing specification

The PV system consists of the Photovoltaic field along with battery storage to storage the power generated by the PV panels. A gas burner is also used in this system which provides the energy when there is a deficit of solar irradiation. This is represented in the following block diagram.

For the sizing, monocrystalline silicon panels were selected with efficiency of 12.5 % and a balance of system efficiency of 8.5 %. The solar PV field provides the power to meet the electric load of 500 kW<sub>e</sub> required by the greenhouse. The area required by the PV to match the electric load was calculated to be approximately 9400 m<sup>2</sup>. The system also consists of a thermal boiler which provides the thermal energy required

<sup>1</sup>The solar multiple is defined as the ratio of the thermal power generated by the solar field at the design point to the thermal power required by the ORC unit at nominal operating conditions.

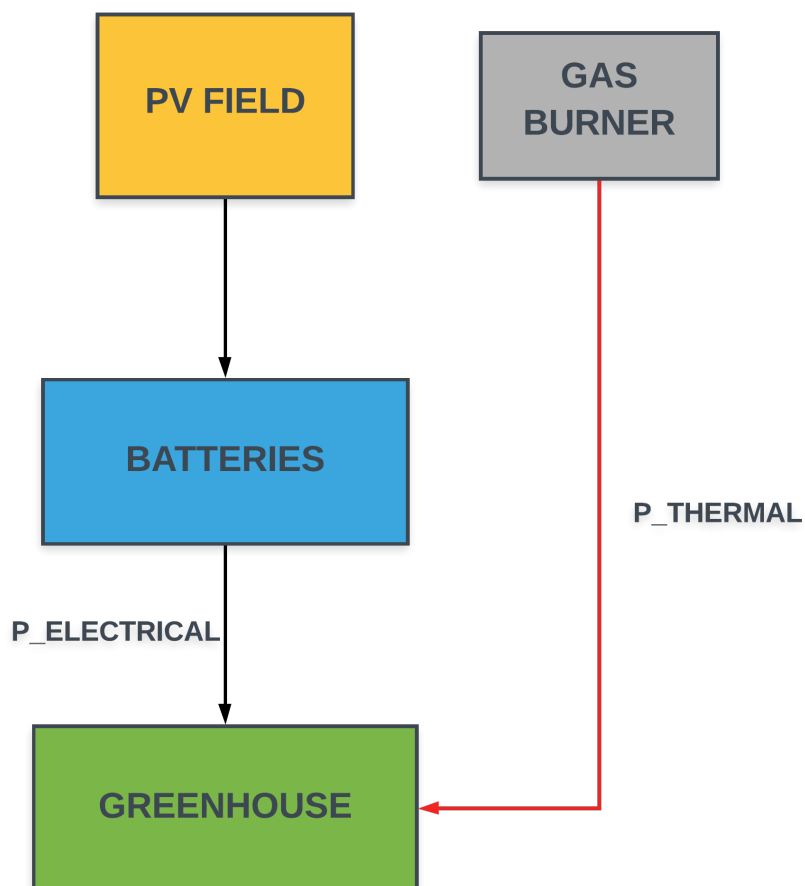


**Figure 2.7:** Block diagram for the PV + gas burner system.  $P_{\text{ELECTRICAL}}$  and  $P_{\text{THERMAL}}$  represents the electrical and thermal power input to the greenhouse.

to meet the thermal load requirements of the greenhouse. The total thermal power delivered by the boiler is  $4500 \text{ kW}_{\text{th}}$  as that is the nominal thermal load required by the greenhouse in winter shown in figure 2.5b. Table 2.2 summarises the technical specifications of components of the photovoltaic system.

	Parameter		Units
<b>PV Specification</b>	Pel	500	kWel
	Peak		
	Balance of system efficiency	0.850	-
	PV nominal efficiency	0.125	-
	PV area	9411.76	m <sup>2</sup>
<b>Battery Storage</b>	Stored energy	5882.35	kWh el
	Peak Power from batteries	500	kWel
<b>Thermal Boiler</b>	Boiler size	4500	kWth
	Thermal energy delivered	90000	kWhth/day
	Gas energetic value	7.222	kWhth/m <sup>3</sup>

**Table 2.2:** Technical specifications for a PV and gas burner system for location in Greece.

### 2.2.3. CAPEX comparison

In this section, the capex of both systems is compared. The capex for both cases is calculated based on current price range. In the case of SPRHOUT, table 2.3 shows that the total calculated CAPEX of 3272000 Euros which includes the cost of installation and all the equipment.

		<b>Cost</b>	<b>Units</b>
<b>ORC CAPEX</b>	ORC Machine	1425.4	€/kW peak
	BoP	20% of ORC cost	kEuros
<b>TES CAPEX</b>	Vessel manufacturing cost	69.354	€/m3
	Vessel BoP	20% of vessel cost	kEuros
	Storage medium cost	1	€/m3
<b>SF CAPEX</b>	Solar collector cost	80	€/m2 aperture
	Structures and BoP	Included	kEuros
	Installation	10	€/m2
<b>Extra Equipment</b>	Intermediary HEX and extra pump	10	kEuros
	Container	30	kEuros
<b>Contingency</b>		10%	%
<b>Total Capex</b>		<b>3272.81</b>	<b>kEuros</b>

**Table 2.3:** Capital expenditure of the SPRHOUT system.

Table 2.4 shows the maintenance expenditure of the solar field and the ORC unit for the SPRHOUT system. The sum of all the operating expenditures gives us the total OPEX of the SPRHOUT system in one year of operation.

	<b>Components</b>	<b>Cost</b>	<b>Units</b>
<b>SF OPEX</b>	Collectors mirror/glass cleaning/ tracking	79.97	kEuros/year
<b>ORC OPEX</b>	ORC system auxiliaries	20.29	kEuros/year
<b>Total OPEX</b>		<b>100.3</b>	<b>kEuros/Year</b>

**Table 2.4:** Operating expenditure of different components in SPRHOUT system.

Table 2.5 the operating expenditures of the different components of the PV + gas burner solution are reported. It can be seen that the OPEX of the PV plant is higher than SPRHOUT system due to the use of a gas thermal boiler to meet the thermal load requirements of the greenhouse.

	<b>Components</b>	<b>Cost</b>	<b>Units</b>
<b>PV OPEX</b>	Collectors mirror/glass cleaning/ tracking	47.06	kEuros/year
<b>Boiler OPEX</b>	Gas	1137.12	kEuros/year
	Maintenance	9	kEuros/year
<b>Total OPEX</b>		<b>1193.17</b>	<b>kEuros/Year</b>

**Table 2.5:** Operating expenditure of different components in PV+gas burner system.

Table 2.6 shows the CAPEX breakdown for the PV+gas burner system. The major

expense is the battery stack. It can be seen that the CAPEX for the PV+gas burner system is more than that of the capital expense of the SPRHOUT system.

		<b>Cost</b>	<b>Units</b>
<b>PV CAPEX</b>	PV field including installation	1400	€/kW peak
	BoP PV field	12% of PV cost	kEuros
<b>Battery Storage CAPEX</b>	Battery pack cost	500	€/kWh
	BoP	12% of battery cost	kEuros
<b>Gas Burner CAPEX</b>	Boiler cost	40	k€/MW
	Gas price	0.25	€/m <sup>3</sup>
	BoP	40% of boiler cost	kEuros
	Container	30	kEuros
<b>Contingency</b>		10%	%
<b>Total Capex</b>		<b>5658.53</b>	<b>kEuros</b>

**Table 2.6:** Capital expenditure of PV + gas burner system.

From this preliminary analysis, the SPRHOUT results cheaper than a PV plus gas burner solution. A detailed analysis simulating the total energy (electricity and heating) generated by the two solutions during one year of operation should be performed in order to correctly identify which solution is more effective. Furthermore, it should be pointed out that the cost of batteries has been decreasing steadily in the past years. If this trend continues the PV system might become more cost effective for matching the energy needs of a large greenhouse facility.



# 3

## Dynamic Model Description

During the past, power plants have been simulated using dynamic modelling software. Application of dynamic models included modelling fossil fuel based and nuclear power plants. This started a phase for the development of dynamic models which would later on be used in various industries such as automobiles, aerospace, thermal plants etc. This chapter gives an overview on dynamic modelling and the open-source modelling language Modelica. It also discusses the open source ThermoCycle library which plays a crucial part in the development of the SPRHOUT library.

### 3.1. Dynamic Modelling and Modelica

Dynamic modelling has been widely applied in the field of power systems. The first softwares to implement dynamic simulations were developed in the mid-20th century. Dynamic simulations were introduced with the aim to better understand the transients characterizing complex power systems in order to better design and optimise such systems. Along with that, virtual prototyping and validation helped to accurately assess the performance of complex systems [23].

Dynamic models based on different level of details can be characterised into two major classes: low order models and detailed physics-based models. The first category is used to implement general control strategies and to study the performance of the system based on general assumptions. This modelling technique is usually used in early phases of a project. Due to the modelling parameters and assumptions being relatively simple, the computational efficiency for such models is quite high. The detailed physics-based model follows the laws of conservation of energy, momentum and mass. Using these laws, the model can accurately describe the system behaviour in conditions which are diverging from the nominal ones. Due to the complex equations used, the computational time for simulations of such dynamic models takes longer.

Modelica is an object-oriented programming language which is largely used for equation based modelling. One of the reasons why Modelica is widely accepted and used in Industries is the ease of use, visual design of models and the ability to model own

libraries for the purpose of simulation. For this thesis, the software Dymola was used for the object-oriented programming.

## 3.2. Solvers used for model simulation

Modelica is used to program a system which can be described with a series of differential algebraic equations (DAE). Differential algebraic equations are a type of differential equations where the derivatives of one or more dependent variables are not present in the set of equations. The variables present without their derivatives are termed as algebraic. The presence of algebraic variables implies the equations cannot be expressed in the explicit form of  $y' = f(t,y)$ .

In order to solve a set of ordinary differential equations (ODE), a numerical integration method along with linear and non-linear solvers are required.

### 3.2.1. DASSL Solver

DASSL is designed for the numerical solution of implicit systems of differential or algebraic equations written in the form  $F(t,y,y')=0$ , where  $F$ ,  $y$ , and  $y'$  are vectors and initial values for  $y$  and  $y'$  are given. System of differential/algebraic equations (DAE) arise in several diverse applications in the physical world. Problems of this type occur frequently in the numerical method-of-lines treatment of partial differential equations, in the simulation of electronic circuits, where they are sometimes called semi-state equations, and in the dynamic analysis of mechanical systems. These problems can all be solved using DASSL. Both a single-precision version (SDASSL) for long word-length machines and a double-precision version (DDASSL) for short word-length machines are included in the software platform Dymola.

## 3.3. ThermoCycle Library Description

This section describes the open source ThermoCycle Library. The Thermocycle library provides a robust framework to model thermohydraulic systems. One of the advantages of the ThermoCycle library is that it functions with non-conventional heat transfer fluids such as refrigerants, ammonia, siloxanes etc. that are used in various components such as heat pumps and Organic Rankine cycle plants.

Thermocycle library is organised into different packages such as [23]:

- **Components**, is categorised into three sub packages: FluidFlow, HeatFlow and Units. Models of heat exchangers, pipes, cells, and control units are all covered in this package.
- **Examples**, includes examples of models where different components of the library are tested.
- **Functions**, includes general mathematical functions along with correlations used in some of the models in the library.

- **Interfaces**, includes the connectors required for different components.
- **Media**, lists the fluids available for simulation in the library.

The structured representation of the library is better shown in the figure 3.1

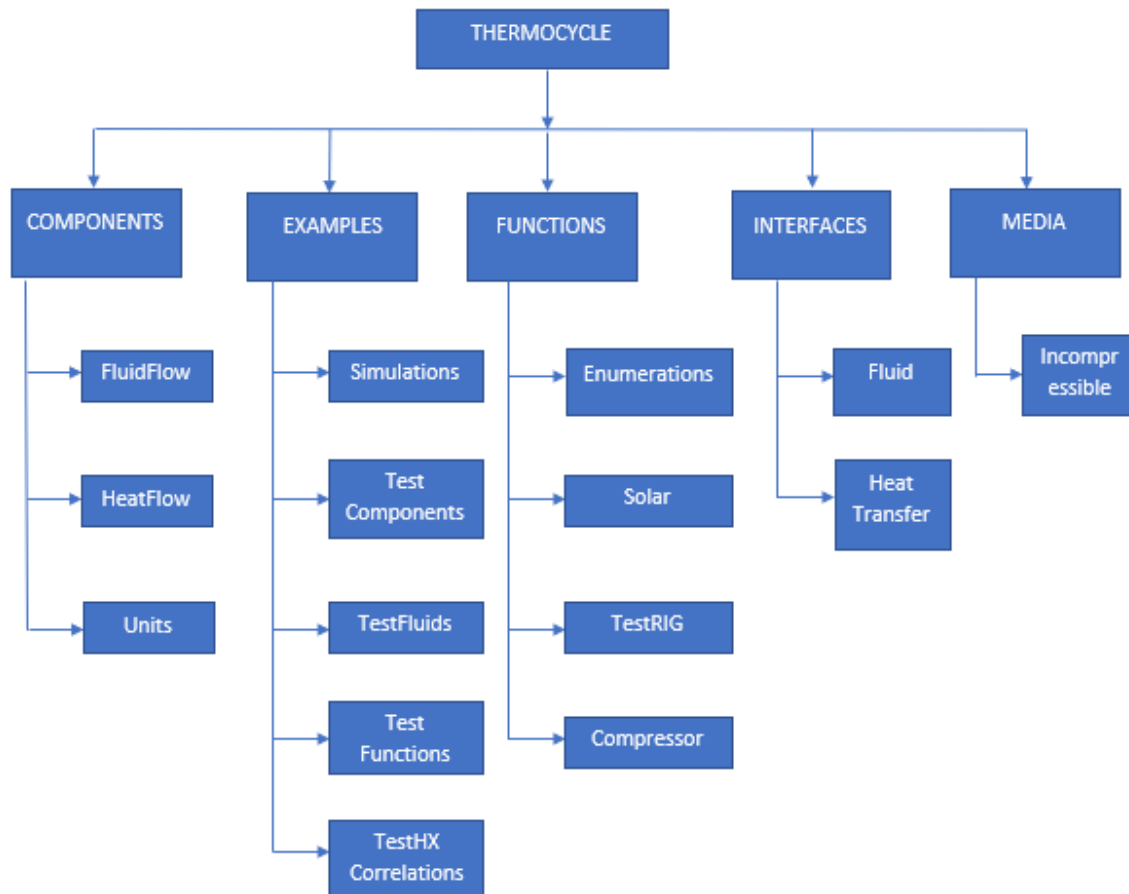


**Figure 3.1:** Schematic representation of the structure of ThermoCycle modelica library.

In the library, the inheritance, class parametrization and enumeration features are used to facilitate the creation of new models. The “Inheritance” feature allows the codes that were already written in a pre-existing model to be reused in another model by extension. The “class parametrization” feature allows the user to define a general class inside a model which is replaceable by different models according to the user requirement.

The “enumeration” feature allows the user to define a collection of items that can be selected according to the requirement of the user, which will change the behaviour of the model. For example, in the case of the SPRHOUT model, the collector model could behave differently with a different set of collector geometries. The different set of collector geometries allowed for the use of multiple collector options thus allowing for greater degree of freedom in terms of selecting the type of collector for the simulation of the model.

In the section below, the core of the ThermoCycle library is described.

### 3.3.1. Cell1DimInc

In order to develop a component model, it is important to start by dividing the model in small cells. The Cell1DimInc model describes the flow of an incompressible fluid through a single cell. By interconnecting several of these cells together, an overall model describing the flow is obtained. The enthalpy is selected as a state variable in this case.

The assumptions made for such a model as listed below.

- Fluid velocity is considered uniform across the cell.
- The pressure is assumed to be constant in the cell.
- The model is based on dynamic energy balance and on a static mass and momentum balances.
- Axial thermal energy transfer is neglected.

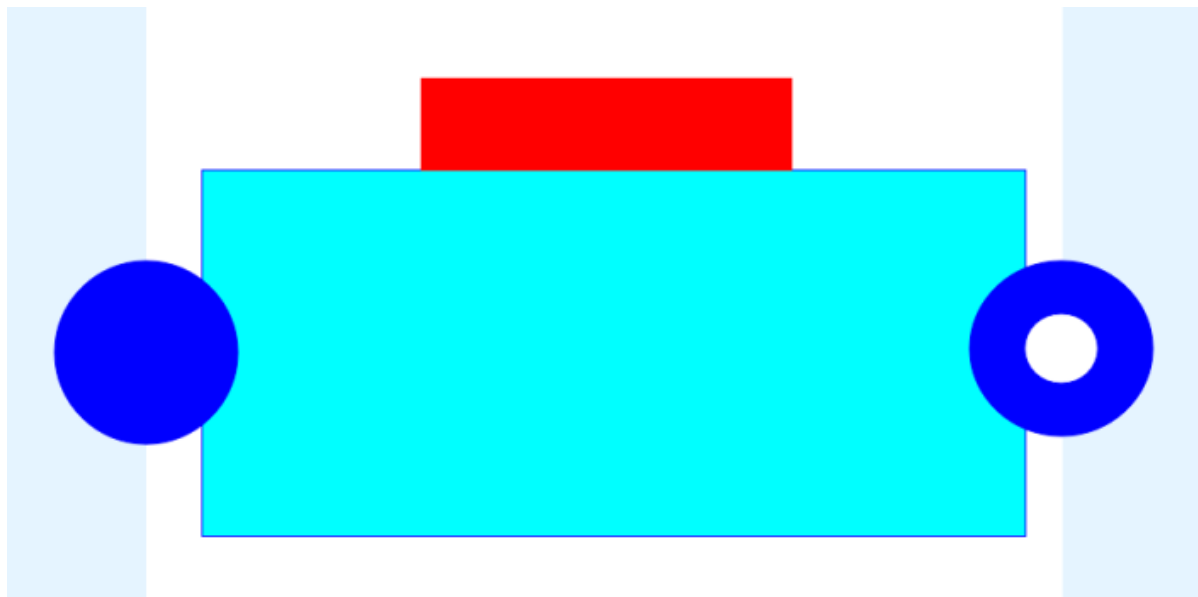


**Figure 3.2:** Schematic representation of Cell1DimInc model in Dymola graphical user interface(GUI).

The figure 3.2 shows the two inlet and exit flow connectors and 1 thermal input block denoted by the red box. The fluid enters from the left hand side via the InFlow connector and exits through the OutFlow connector on the right.

### 3.3.2. Flow1DimInc

Flow1D model computes the heat transfer in the fluid flowing through the heat absorbing tubes. It is based on one-dimension (1D) dynamic mass and energy balance, discretized with the finite volume method and static momentum balance. One of the assumptions of this model is that the fluid entering is incompressible and pressure remains constant throughout the model.

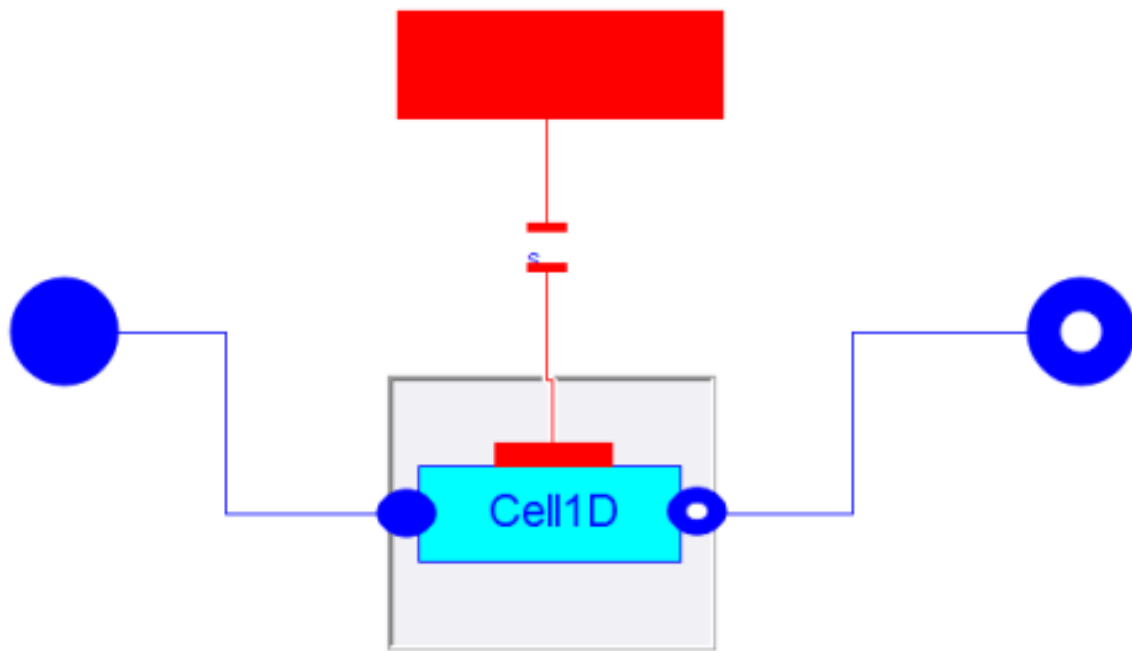


**Figure 3.3:** Schematic representation of Flow1DimInc model in Dymola graphical user interface(GUI).

The figure 3.3 shows the inlet and outlet ports along with Cell1Dim connected to the thermal port.



# 4

## SPRHOUT Modelica Model

As discussed in the chapter 3, the SPRHOUT Modelica model is developed based on the Modelica programming language. The SPRHOUT library was developed based on the ThermoCycle library. The intended purpose of this chapter is to give the reader an overview of the SPRHOUT library and describe the different components used for the simulation of the SPRHOUT system.

### 4.1. SPRHOUT Library

The SPRHOUT library is designed specifically to represent the SPRHOUT unit developed by SOLHO, and it is organised into different packages such as:

- **Components**, which is further categorised into five sub packages: Data, Solar collector, Power block, TES, and Control unit.
- **Interfaces**, includes the connectors required for different components.
- **Media**, lists the fluids available for simulation in the library.
- **Functions**, which includes general mathematical functions along with correlations used in some of the models in the library.
- **Test simulations**, includes the framework where the SPRHOUT can be simulated.

An illustration of the main packages and sub-packages included in the SPRHOUT library are represented by the figure 4.1

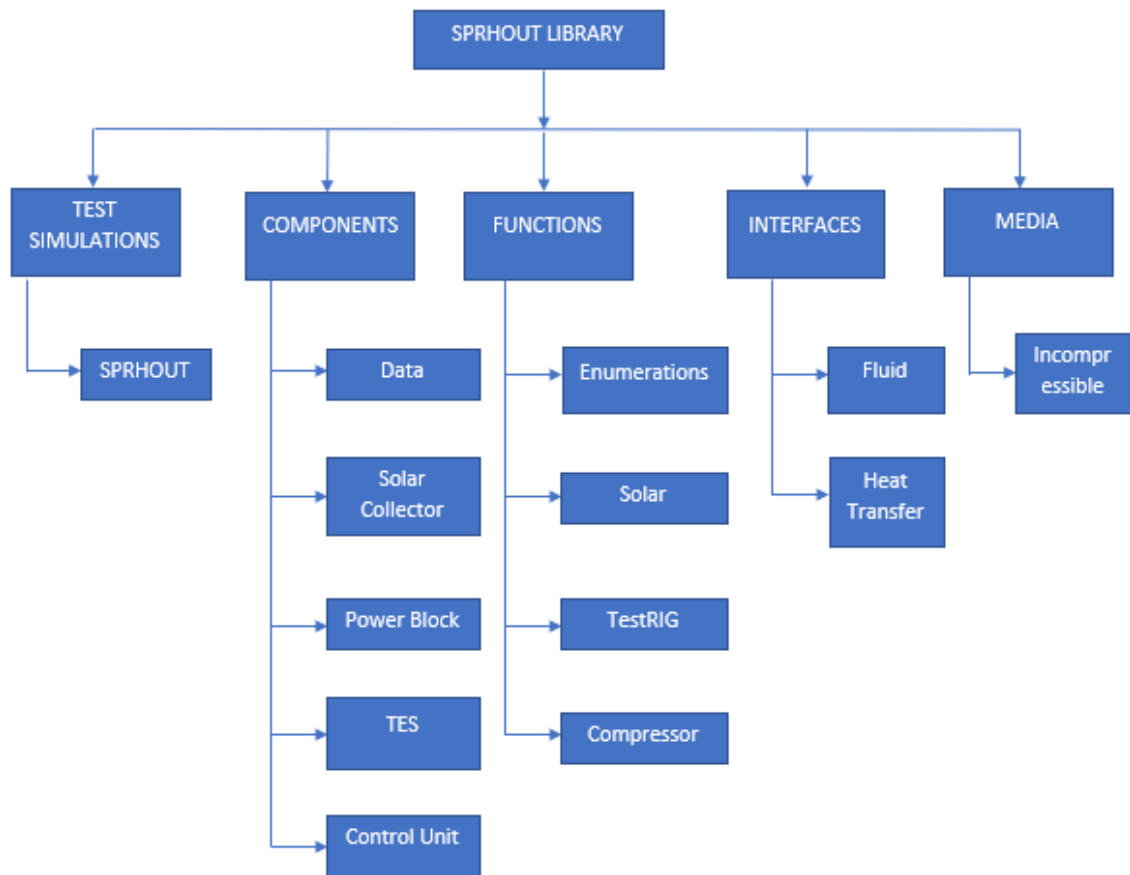


**Figure 4.1:** Schematic representation of the structure of SPRHOUT modelica library.

## 4.2. SPRHOUT component description

This section describes the various components used in the SPRHOUT system. The SPRHOUT model is based on the connection of different models of a flat plate solar collector field, a thermal energy storage, a gas burner, a power block based on the Organic Rankine Cycle (ORC) and a control unit.

### 4.2.1. Flat plate solar collector

The flat plate solar collector model allows for a one-dimensional (1D) discretization of the heat absorbing tubes. The model consists of two sub-components: Flow1DInc model and the AbsFlatPlate model. Flow1DInc model computes the heat transfer in the fluid flowing through the heat absorbing tubes. As the fluid is always in liquid state, incompressibility is assumed in the collectors. The connection between the two components is ensured by a thermal port as shown in Figure 4.2.

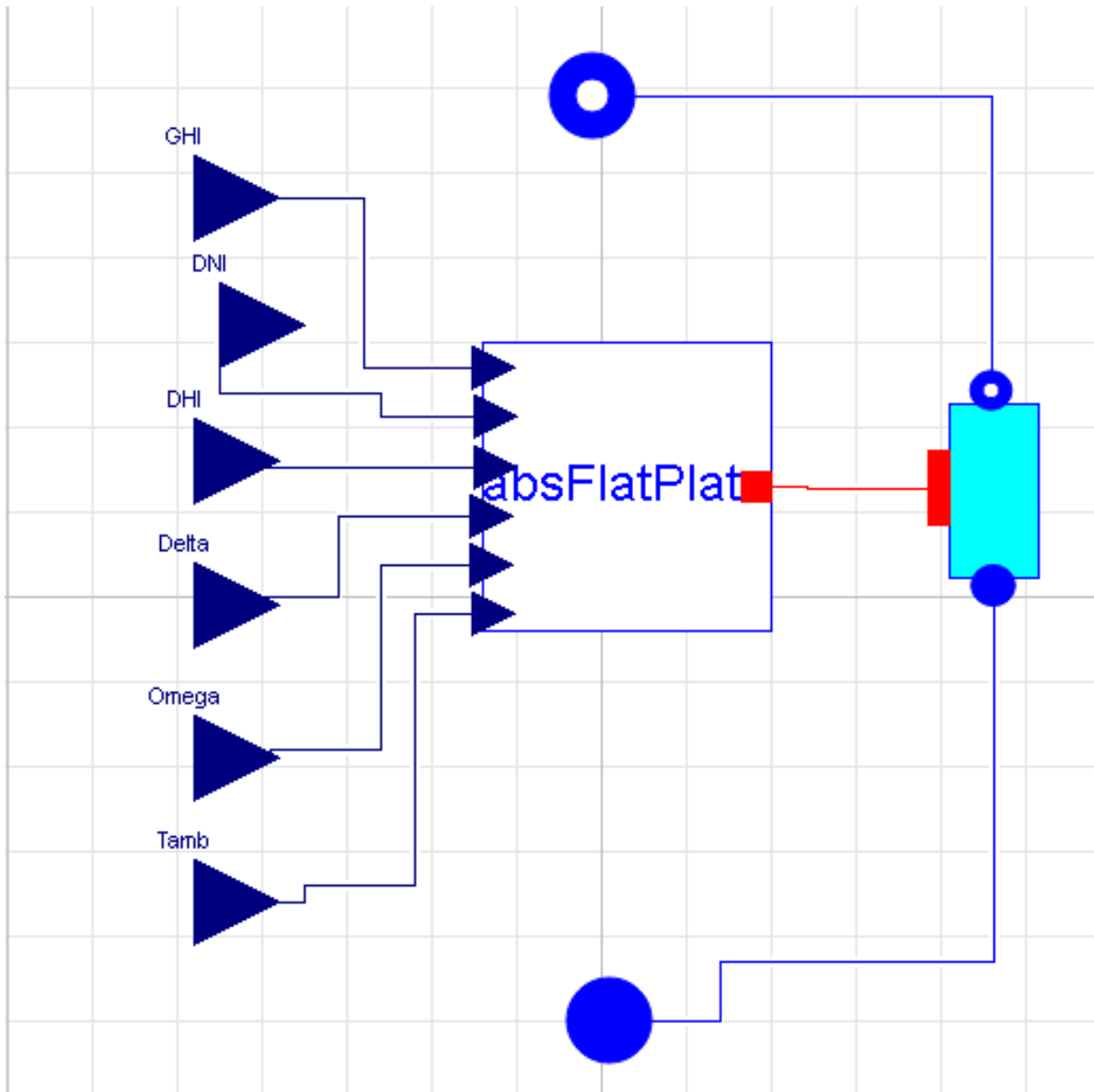


**Figure 4.2:** Diagram of flat plate solar collector model from Dymola graphical user interface (GUI). The model is composed of AbsFlatPlate model connected with the Flow1Dim model.

The AbsFlatPlate model calculates the irradiation received on the tilted flat panel. The model implements the relation between different environmental factors: the Global Horizontal Irradiance ( $GHI$ ), the Direct Normal Irradiance ( $DNI$ ), the Direct Horizontal Irradiance ( $DHI$ ) along with the solar declination angle  $\delta$ , the hour angle  $\omega$  the ambient temperature  $T_{amb}$  and the temperature distribution along the absorber,  $T_m$ . The ambient data taken as an input are of the  $TMY$  [Typical Meteorological Year] type [24].

The angle of incidence of beam radiation on a surface at angle theta, is related to other angles, by equation 4.1,

$$\begin{aligned} \cos\theta = & \sin\delta\sin\phi\cos\beta - \sin\delta\cos\phi\sin\beta\cos\gamma + \cos\delta\cos\phi\cos\beta\cos\omega \\ & + \cos\delta\sin\phi\sin\beta\cos\gamma\cos\omega + \cos\delta\sin\beta\sin\gamma\sin\omega \end{aligned} \quad (4.1)$$

where  $\gamma$  is the azimuth angle.

The incident beam radiation ( $W/m^2$ ) is calculated as,

$$I_b = DNI * \cos\theta \quad (4.2)$$

The irradiation on the tilted panel ( $IT$ ) is then computed as,

$$IT = I_b + I_d * \left(\frac{1 + \cos\theta}{2}\right) + GHI * (\rho.g) * \left(\frac{1 - \cos\theta}{2}\right) \quad (4.3)$$

where  $I_d$  is the diffused horizontal irradiation and  $\rho.g$  is the albedo factor.

Finally, the efficiency of the solar collector ( $\eta$ ) is based on an experimental equation derived by the manufacturer [25], as follows,

$$\eta = \eta_0 - a_1 * \frac{T_m - T_{amb}}{IT} - a_2 * \frac{(T_m - T_{amb})^2}{IT} \quad (4.4)$$

where  $\eta_0$  is the standard efficiency of the panel,  $T_m$  is the mean fluid temperature in °C,  $T_{amb}$  is the ambient temperature in °C and  $a_1$  and  $a_2$  are constants specified by the manufacturer having the units ( $W/m^2K$ ) and ( $W/m^2K^2$ ) respectively.

### 4.2.2. Thermal Energy Storage (TES)

Thermal Energy Storage is the key component of the SPRHOUT system as it allows the greenhouse to operate off-grid. The Thermal energy storage is based on the principle of flow storage where the heat transfer fluid (*HTF*) used to store the heat, can be water, thermal oil or molten salt, depending on the operating temperatures. In the so-called *direct systems*, the heat transfer fluid also serves as the storage medium. In *indirect systems*, a different medium is used as storage.

The proposed solution is a thermocline storage in which hot and cold fluid enters and exits at the top and at the bottom of the storage respectively. The TES uses water as the heat transfer fluid which can be altered to include different HTFs and filler materials according to the needs of the greenhouse facility.

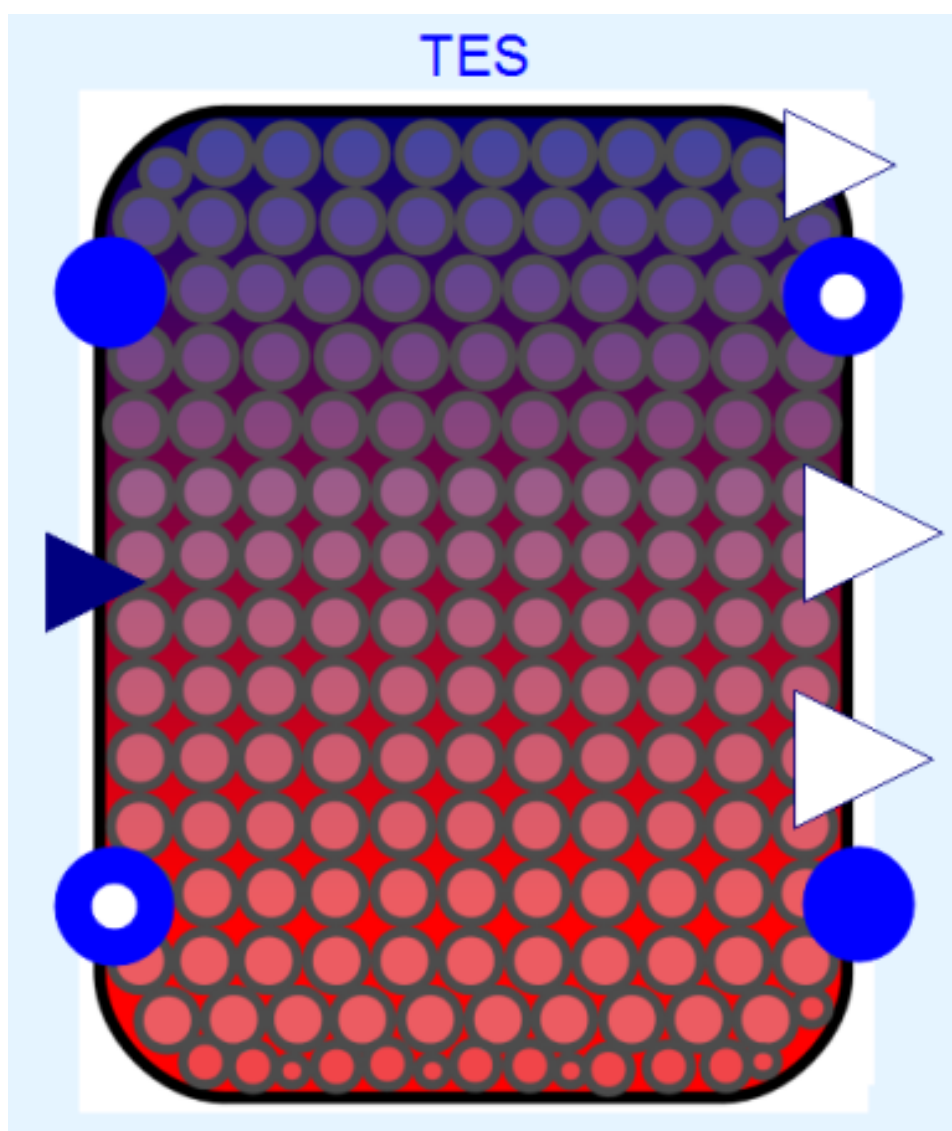


Figure 4.3: Schematic representation of TES block in Dymola.

The storage characteristics are defined based on its capacity and its operating temperatures.

The TES model stores the thermal energy coming from the solar collector field as sensible heat which is then used to power the Organic Rankine Cycle power block.

The TES model is designed to keep the volume of the container constant while the pressure is variable. The model is based on the mass and energy balance equations along with momentum conservation. The energy balance of the thermal storage system [20] can be expressed in a general form as shown by the equation 4.5.

$$(\rho.C_p)_{eff} \cdot \frac{\partial T}{\partial t} + \epsilon \cdot (\rho.C_p)_{liquid} \cdot v_{liquid} \cdot \frac{\partial T}{\partial z} = k_{eff} \cdot \frac{\partial^2 T}{\partial z^2} - U_w \cdot a_w \cdot (T - T_\infty) \quad (4.5)$$

where  $\rho$  is the density of liquid (kg/m<sup>3</sup>),  $C_p$  is the heat capacity (J/kg.K),  $\rho C_p$  is the volumetric heat capacity (J/m<sup>3</sup>K),  $k_{eff}$  is the thermal conductivity (W/mK),  $v_{liquid}$  is the velocity of the liquid (m/s),  $U_w$  is the coefficient of thermal losses to the environment (W/m<sup>2</sup>K) and  $a_w$  is the ratio between thermal loss area and tank volume.

### 4.2.3. Power Block

The power block converts the thermal energy from the TES into electricity and is based on the Organic Rankine Cycle (ORC) technology. As the dynamics characterizing the power unit are small compared to TES and the solar field, the model was developed using algebraic equations. Only the dynamics of the evaporator are considered where the mass flow rate and temperature change are taken into account along with the enthalpy.

Figure 4.4, the power block from the Dymola graphical user interface is shown. The power block model was developed to match the electric load requirement of the greenhouse. The top left and bottom left ports represent the inlet and outlet for the fluid to enter and exit the power block.

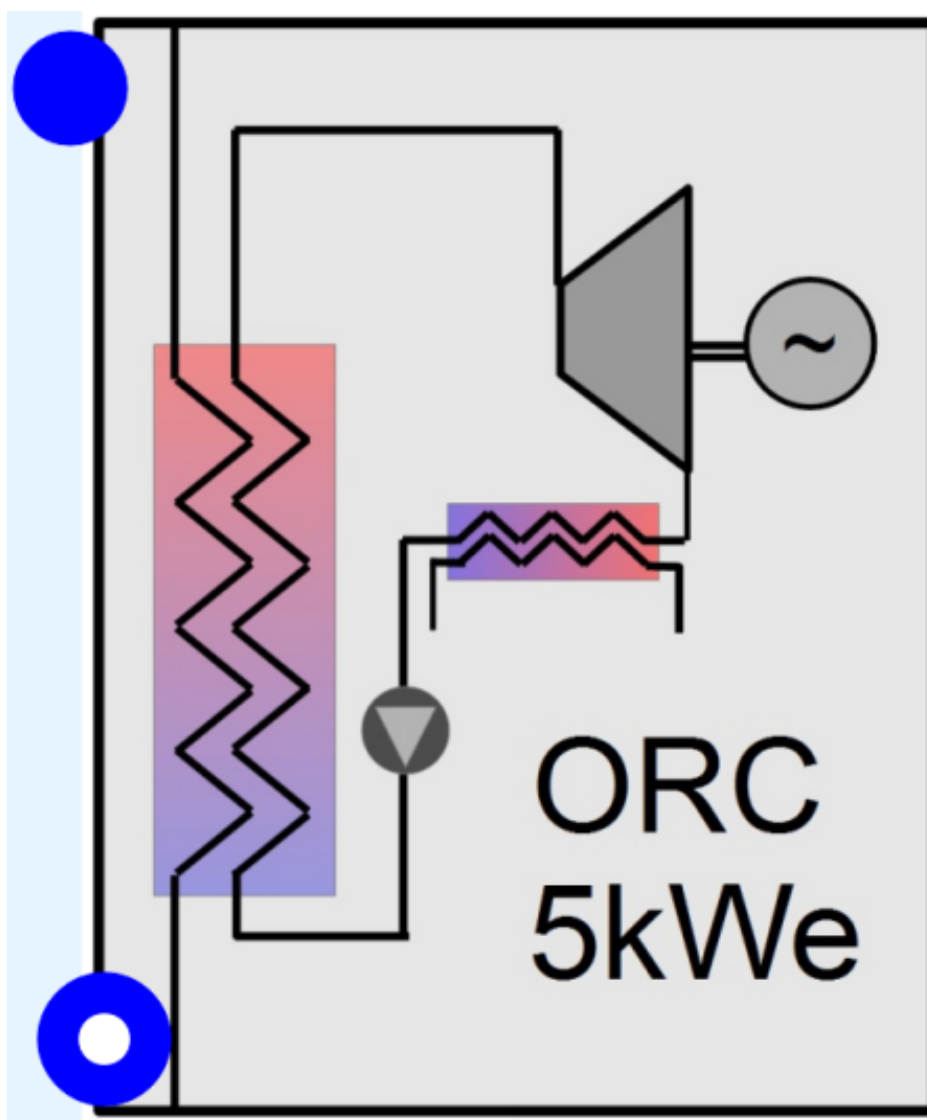


**Figure 4.4:** Representation of the Power Block model from the Dymola graphical user interface (GUI).

#### 4.2.4. Control Unit

The control unit consists of the equations describing the control logic of the SPRHOUT. The model includes a block to simulate the Proportional integral controller used to stir the solar field the mass flow rate by acting on the solar field pump rotational speed. The control strategies are discussed in detail in the next chapter.

The proportional-integral controller consists of a proportional gain along with an integrator. The proportional gain provides a fast error response. The higher the value, the faster is the system response to the error. The role of the integrator is to guide the system towards a zero steady-state error. Figure 4.5 represents the PI block used in the SPRHOUT control unit.

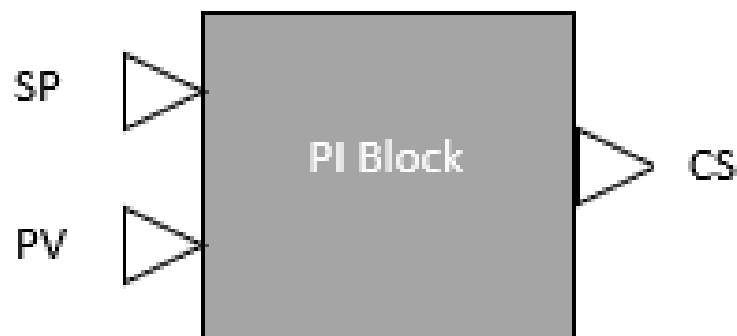


**Figure 4.5:** Block representation of the PI controller model used in Dymola.

In the PI model, the controller output  $u(t)$  is fed into the pump which controls the mass flow rate through the solar field.

$$e(t) = SP - PV \quad (4.6)$$

$$u(t) = u_{bias} + K_c \cdot e(t) + \frac{K_c}{\tau} \int_0^t e(t) \cdot dt \quad (4.7)$$

The two important parameters for tuning in a PI controller are the proportional gain  $K_c$  and the integral time  $\tau$  which is represented in the equation 4.7. As discussed above, if the value of the proportional gain is high, the controller is more aggressive at responding to errors away from the desired set-point (SP). The error,  $e(t)$  is calculated as the difference between the set-point and the process variable (PV), which is represented by the equation 4.6.

#### 4.2.5. Gas Burner

The gas burner model was introduced in order to maintain the temperature at the outlet of the solar field at the defined limit of 90°C when the irradiation is insufficient. A

simplified approach is adopted to simulate the gas burner. The gas burning process is modelled as a zero- dimensional model where the power from the biomass combustion is imposed by the user. The fluid side is modelled with a discretized one- dimensional approach. The fluid flow through the boiler is modelled with a Flow1Dim component, accounting for energy accumulation. The thermal inertia of the boiler is neglected as being considerable smaller than the one characterising the dynamics of the fluid side.

The controller decides the input value using the following equation:

$$Q_{burner} = \dot{m} \cdot C_p \cdot (90 - TT002) \quad (4.8)$$

Where the  $\dot{m}$  is the mass flow set by the pump P001,  $C_p$  is the specific heat capacity in kJ/kg.K and TT002 is the temperature at the outlet of the solar field in °C.

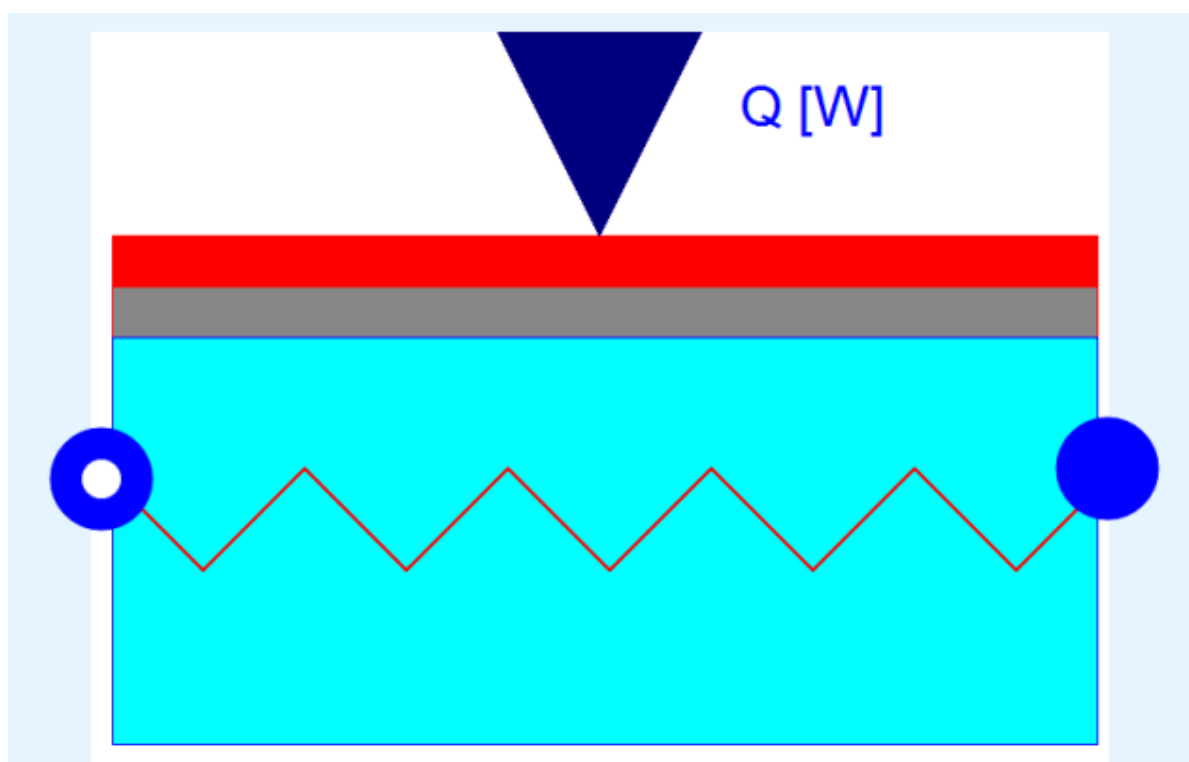


**Figure 4.6:** Representation of the gas burner model from the Dymola graphical user interface (GUI).

When the required energy provided by the solar field is not enough, the deficit energy is calculated by the controller and fed into the gas burner model which heats up the working fluid before it enters the thermal energy storage. This ensures that whenever required, the gas burner can act as a backup energy source.

### 4.2.6. Expansion Tank

The expansion tank is a small tank that allows defining the working pressure in the hydraulic circuit. As the fluid inside the thermal storage expands thermally due to heat, the excess fluid is stored in the expansion tank thus keeping the pressure constant.

The expansion tank is divided in two parts by a rubber diaphragm. One side of the tank is connected to the heating vessel and stores the working fluid. The other side contains pressurised air. This helps in maintaining the pressure inside the heating vessel at the desired level.

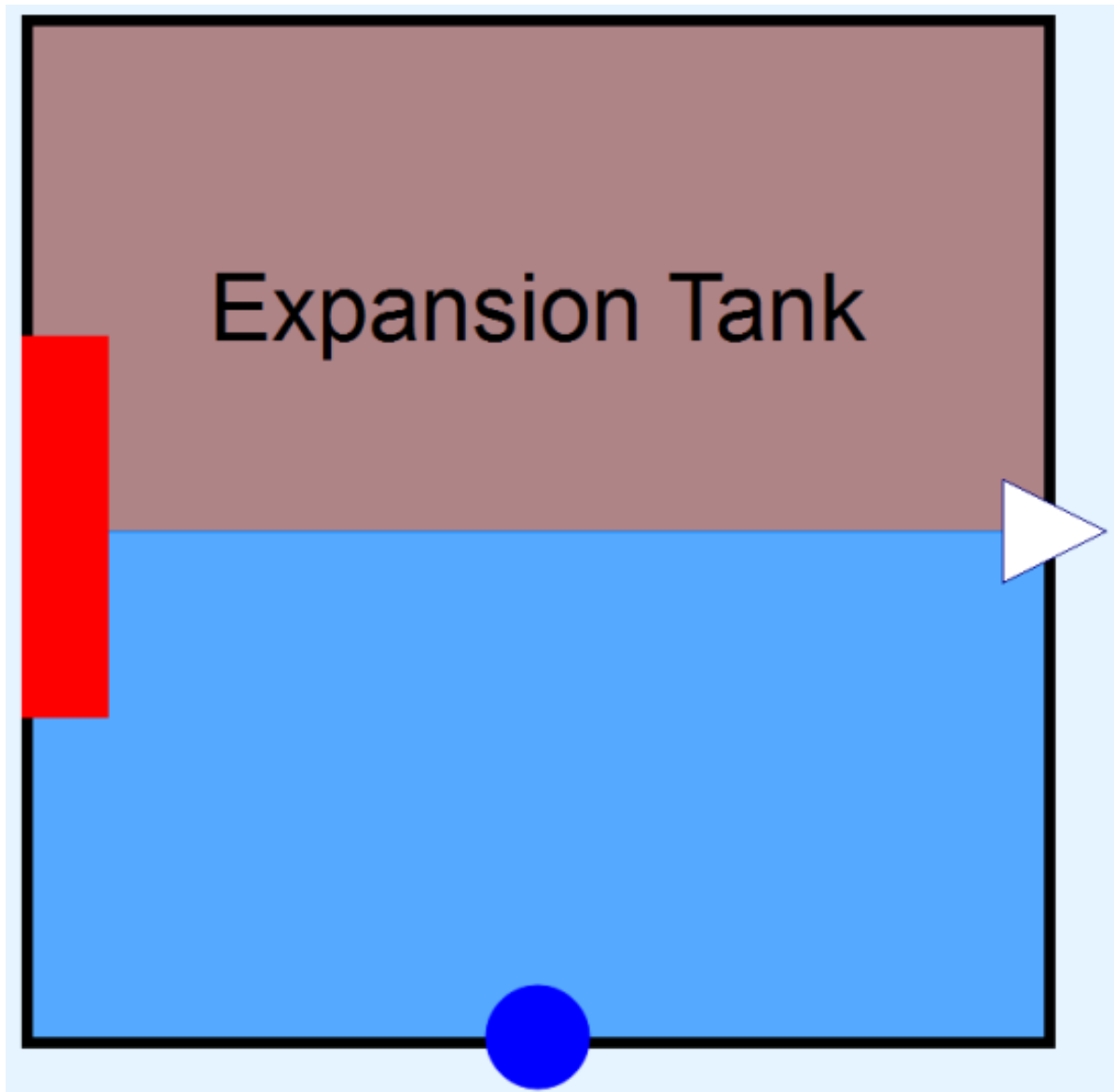


**Figure 4.7:** Representation of the Expansion tank model from the Dymola graphical user interface (GUI).

For the model, the enthalpy and pressure are selected as state variables. The pressurised air is considered ideal and follows Boyle's law which states that the absolute pressure exerted by a mass of gas is inversely proportional to the volume that the gas

occupies for a given temperature and amount of gas in a closed system. It can be summarised by the following equation:

$$PV = k \quad (4.9)$$

where P is the pressure of the gas, V is the volume of the gas and k is a constant.

Another assumption for the expansion tank model is that the gas is considered to be at the same temperature as that of the working fluid.

#### **4.2.7. Fan**

The fan model is modelled on similar principles as the gas burner. The fan simulates the thermal energy input required for the greenhouse. The fluid flow through the fan is modelled with a Flow1Dim component, accounting for energy accumulation.

The fan model and gas burner models have the same functions with a minor difference. In this model, the heat is taken out of the system to simulate heat being imparted to the greenhouse. In case of the gas burner, the thermal heat was used as an input to heat up the working fluid.

### 4.3. SPRHOUT Overview

This section gives the overall layout of the SPRHOUT system and how all the components are interconnected together in the Modelica simulation environment.

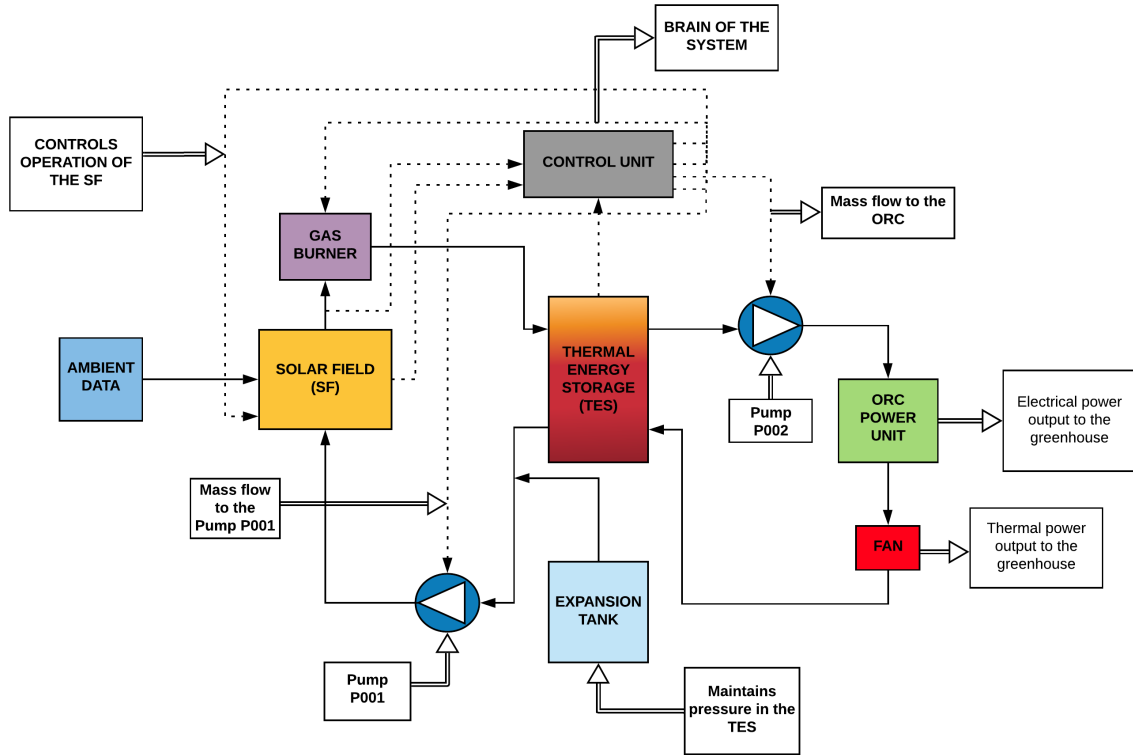


**Figure 4.8:** Representation of the SPRHOUT model used for simulation in Dymola.

The figure 4.8 shows the different components and their interconnections. It can be seen from the figure that the fluid flows from the SF to the TES unit via the gas burner. The input to the gas burner is controlled by the control unit which also controls the mass flow rates through pumps P001 and P002. The ORC power unit provides the electrical power and the fan simulates the thermal power.

# 5

## Control Strategies

In order for the SPRHOUT to work effectively, an optimised control strategy needs to be developed. This chapter discusses the different control strategies that were developed and the optimised control strategy that is used in the final simulation of the system. Finally, the model input data and the simulation parameters are described.

### 5.1. Initial Control Strategy

The main aim of the SPRHOUT system is to help meet the load requirements of the greenhouse. The initial control strategy focuses on the electrical and thermal loads of the greenhouse. One of the first assumptions made for the initial strategy is to check the electrical load first and with respect to the electrical load, control the energy produced by the plant. The flow chart for the initial control strategy is represented by the figure 5.1.

If the irradiation received by the solar field is greater than the threshold irradiation, then the system performs a check on the energy stored in the thermal energy storage. If the irradiation is less than the threshold, then solar field is turned off, i.e. basically turning off the pump of the solar field. It is also necessary that the energy inside the TES is sufficient to run the Organic Rankine Cycle (ORC) power unit for a minimum of 1 hour. If the condition is met, then the ORC power unit is switched on. Otherwise, a check is made if the temperature at the exit of the solar field is 90°C according to which the gas burner will be turned on or off.

Finally, the energy produced is compared to the load required. If the energy produced is in excess of the load, then energy needs to be dumped and vice versa. The thermal load is also checked according to which the fan is turned on or off.

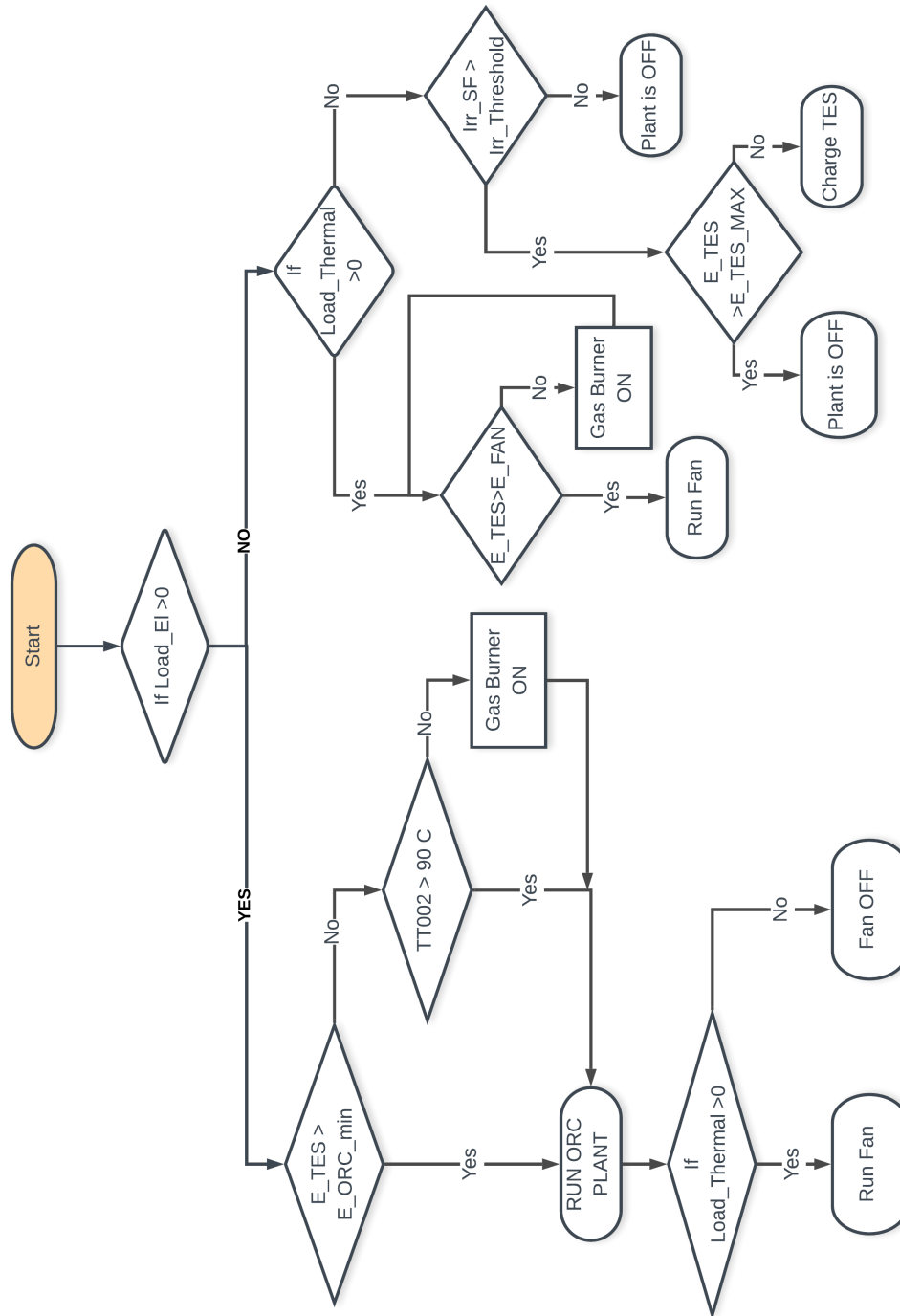


**Figure 5.1:** The initial control flow chart. The initial check is for the load represented by  $Load_{EI}$ .

There were some limitations with this control strategy. The goal was to ensure that the temperature at the outlet of the solar field was at 90°C, but this strategy doesn't take into account when the TES is full or not. The solar field was in an ON state even when the TES was completely charged, resulting in temperatures rising higher than 100°C. Also the use of the gas burner was not optimised as there were times the gas burner was in an ON state even when it was not required.

This required an update in the control strategy in order to check the better functioning of the system. The next section discusses the strategy.

## 5.2. Final Control strategy

As discussed in the previous section, the initial control strategy didn't take into account the energy in the TES at any given point. This meant even when the TES was full, the solar field was providing thermal energy to the TES causing the temperatures in the TES to rise above the set operating temperature of 90°C. This was rectified in the final control strategy which can be seen in figure 5.2.

Similar to the initial control strategy, the first step is to check whether the electrical load is required by the greenhouse. Following that, the next check for the solar field. When the irradiation is not above the threshold irradiation, the SF is in an OFF state. The threshold irradiation is defined as the minimum irradiation required to raise the temperature of the fluid inlet at the SF from 70° to 90°C at the outlet of the SF. From the calculations, it was found that the minimum irradiation required was approximately 340 W/m<sup>2</sup>. If the irradiation is less than the threshold irradiation, the next check on the energy in TES is performed.

The energy in TES at a given point is compared with respect to the maximum energy that can be stored in the TES. The condition was be seen as follows,

$$E_{TES} < E_{TES-max} \quad (5.1)$$

If the given condition is satisfied, the solar field SF is in an ON state. In the case that the TES gets full, the SF is turned OFF.

One of the important parameters is to schedule when the ORC power plant runs. In order to do so, a condition is set that minimum energy required to run the power plant should be atleast equal to the energy required to run the plant for 1 hour. With this condition, the control of the power block becomes simpler and more accurate compared to the previous control strategy. In case the energy in the thermal energy storage is less than the threshold required to run the ORC plant, then another check is performed. This check studies the temperature at the outlet of the solar field. If the temperature at the outlet is not 90°C, it implies that the irradiation is not enough to charge the TES and thus run the ORC plant. In such a case, the alternative is to use the backup gas burner to charge the TES and successfully run the ORC. The final check to see if thermal load is required. If it is not, then the fan is in OFF state. Otherwise the fan is turned ON to match the thermal load requirement of the greenhouse.

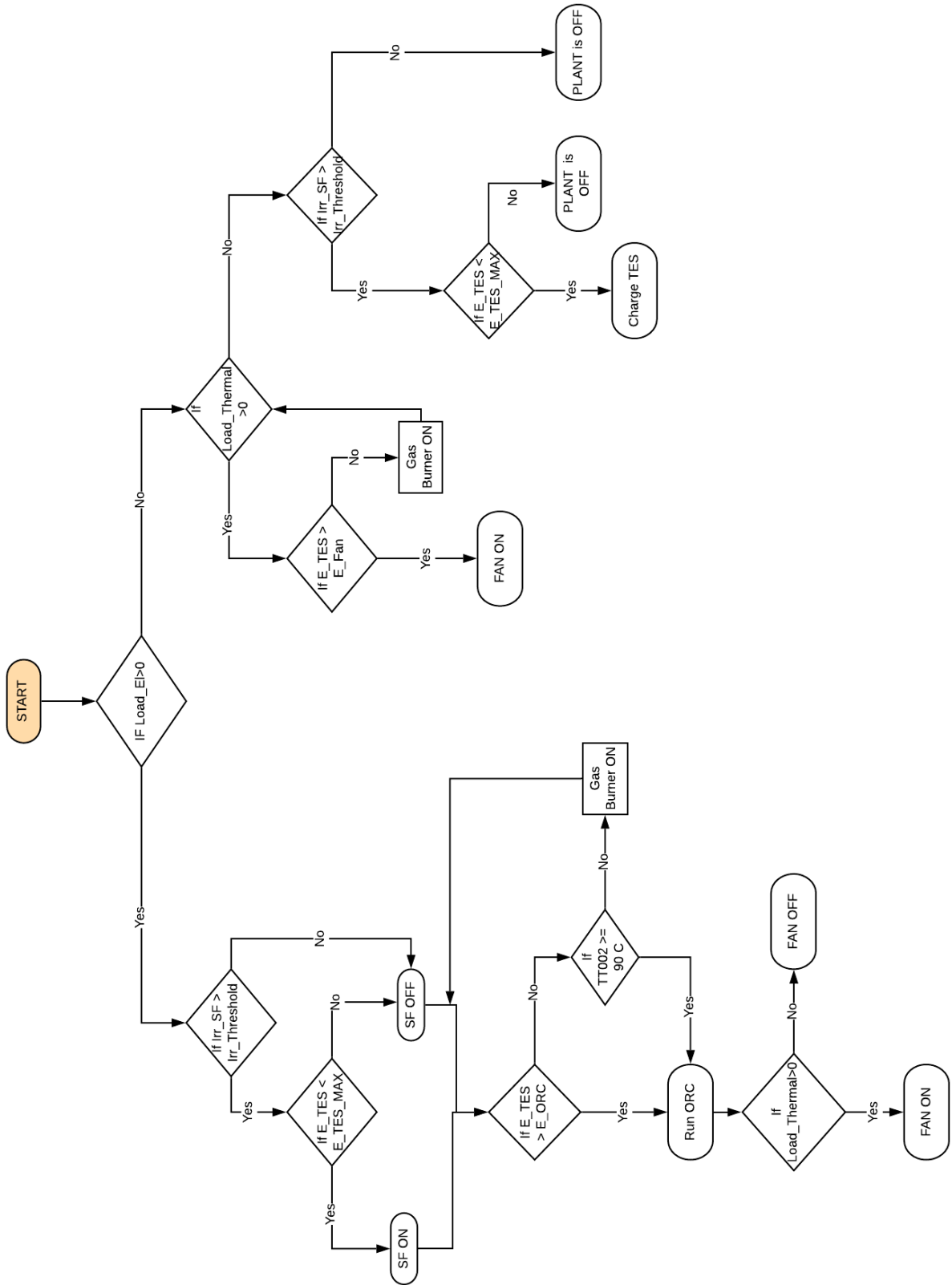


Figure 5.2: The final control flow chart. The initial check is for the load represented by Load<sub>EI</sub>.

# 6

## Simulation Results and Discussion

This chapter reports the results obtained by simulating the SPRHOUT Modelica model. The model was run to investigate the control logic on a daily basis and the control strategies on an annual basis. The first section presents the initial conditions of the model inputs and parameters for the control logic analysis and the economic analysis. The second section discusses the results from the control logic analysis and finally the SPRHOUT economic analysis results are reported in the third section.

### 6.1. Model Inputs and parameters

This section describes the model input and parameters for the two different analysis performed: the control logic analysis and the SPRHOUT economic analysis.

#### 6.1.1. Control logic analysis

The case study for the control logic analysis was done taking a 1 kWe SPRHOUT system. As described previously, the ambient data selected was the TMY (Typical Meteorological Year) data for Jeddah in Saudi Arabia. In order to make the simulation faster, a moving average was used on the ambient data. The data was calibrated in such a way that the final data for a month represented 24 hours, with each hour averaged for the whole month. For example, the 1 am hourly data for each day of the month was averaged. This was done for all the 24 hours in the day. Thus, for the final simulation, 12 curves were present representing the 12 months of the year.

Using this ambient data, the SPRHOUT system was simulated for 1 year. The initial conditions for the different components are reported below.

Table 6.1 presents the solar field input parameters used for the simulation of the SPRHOUT.

It can be seen from the table 6.1 that the flat plate collector was modelled to have 3 cells per collector. A total of 8 panels were used for the initial simulation where the model was simulated for a 1 kW electrical load for the greenhouse. Based on the load

Parameter	Value
Medium	Water
Number of cells per collector	3
Number of collectors in series	4
Number of collectors in parallel	2
Total nominal mass flow (Kg/s)	0.72
Collector type	Single glazed flat plate collector
Inlet temperature (°C)	70
Outlet temperature (°C)	90
Pressure (bar)	1.2
Heat transfer coefficient (W/m <sup>2</sup> K)	300

**Table 6.1:** Solar field model parameters.

data, the total nominal mass flow was calculated to be 0.72 Kg/s. A total of 8 panels were used with 2 rows of 4 series-connected panels in parallel to provide the heat to the thermal energy storage. It should be noted that the parameter values have to be adjusted with the increase in the area of the greenhouse. This implies, with higher electrical and thermal loads, the area of the solar field will increase and hence the nominal mass flow as well.

For the thermal energy storage (TES) model, the parameters are reported in Table 6.2.

Parameter	Value
Medium	Standard Water
Number of Nodes	21
Number of Sensors	6
Volume of tank [m <sup>3</sup> ]	10.27
Height of tank [m]	1.14
Total nominal mass flow [Kg/s]	0.72
Heat transfer coefficient (W/m <sup>2</sup> .K)	300
Pressure (bar)	1.2
Inlet Temperature (°C)	70
Outlet Temperature(°C)	90
Filler porosity	1
Fluid thermal conductivity (W/m.K)	0.609

**Table 6.2:** TES simulation parameters

As can be seen from the table, the TES is divided into 21 different nodes in order to study the thermocline effect in an effective way.

Similarly, for the control block model, the input parameters are shown in table 6.3.

In case of SPRHOUT, the desired set-point is the temperature at the outlet of the solar field (SF), that is set at 90°C. The final control signal, which is the value of the mass flow rate in kg/s, that is sent to the pump which controls the flow so that the temperature

Parameter	Value
$K_p$ (normalised units)	-4
Ti (s)	12
PVmin ( $^{\circ}\text{C}$ )	10
PVmax ( $^{\circ}\text{C}$ )	95
CSmin (Kg/s)	0.0001
CSmax (kg/s)	8
PVstart( $^{\circ}\text{C}$ )	10
CSstart (Kg/s)	0.6

**Table 6.3:** PI control parameters

at the outlet of the SF is at the desired set-point defined by the user. Table 6.3 shows the final values of the parameters used for the PI control block. PVmin and PVmax refers to the minimum and maximum value of the process variable. Similarly, CSmin and CSmax implies the minimum and maximum values of the control signal.

Parameter	Value
Medium	Water
Volume of Tank ( $\text{m}^3$ )	1
Total nominal mass flow (Kg/s)	0.72
Inlet temperature of tank ( $^{\circ}\text{C}$ )	70
Constant Pressure value (bar)	1.2

**Table 6.4:** Expansion tank parameters

Table 6.4 represents the expansion tank model parameters used for the simulation of SPRHOUT. It can be seen that for a  $1 \text{ kW}_{el}$  load, the volume of the expansion tank is  $1 \text{ m}^3$  which was finalised by calculating the change in volume when the fluid expands as the temperature rises from  $70^{\circ}\text{C}$  to  $90^{\circ}\text{C}$  in the TES.

### 6.1.2. Economic analysis

A case study was defined in order to perform the economic analysis. In particular, the study was performed considering a greenhouse facility in Jeddah, Saudi Arabia. The main assumptions and data are summarised as follows:

- An electrical load of  $50 \text{ kW}$  was considered with the area of the greenhouse to be  $7150 \text{ m}^2$ .
- Tomato was selected as the product that is cultivated in the greenhouse for the purpose of this study. The specific yield was assumed to be  $85 \text{ Kg/m}^2/\text{year}$ .
- The ambient data selected was the TMY (Typical Meteorological Year) type which would provide accurate data for the irradiation received at that location.
- The Thermal Energy Storage unit was designed to provide approximately 12 hours of independence or backup when fully charged.

In order to investigate the economic performance of the SPRHOUT system, the Net Present Value (NPV) and Payback Time (PBT) were selected as the two indicators.

The payback time was calculated using the following expression,

$$PBT = IC/AS \quad (6.1)$$

Where IC is the total investment cost and AS is the total annual savings.

The NPV is computed as,

$$NPV = \sum_{t=1}^n \frac{R_t}{(1+i)^t} \quad (6.2)$$

Where,  $R_t$  is the Net cash inflow – outflows during a single time period,  $i$  is the real rate and  $t$  is the time period. The real rate which accounts for the discount rate and the inflation rate for this case study is calculated to be 7.10%.

This can also be represented as,

$$NPV = \text{sum}(NPV_i) - CAPEX \quad (6.3)$$

where CAPEX is the capital expenditure incurred at the start of the investment period and  $NPV_i$  is the net present value for each year.

The net cash inflow  $R_t$  is computed as,

$$R_t = AR - OPEX \quad (6.4)$$

where AR is the annual revenue in kEuros which is the cost that is saved by not burning gas and buying electricity from the grid. The OPEX is the operating cost of the system.

## 6.2. SPRHOUT control logic analysis

The SPRHOUT system was tested for a simulation of a greenhouse with an electrical load requirement of  $1 \text{ kW}_{el}$ . As described previously, the ambient data selected was the TMY (Typical Meteorological Year) data for Jeddah in Saudi Arabia. The model was simulated for one year.

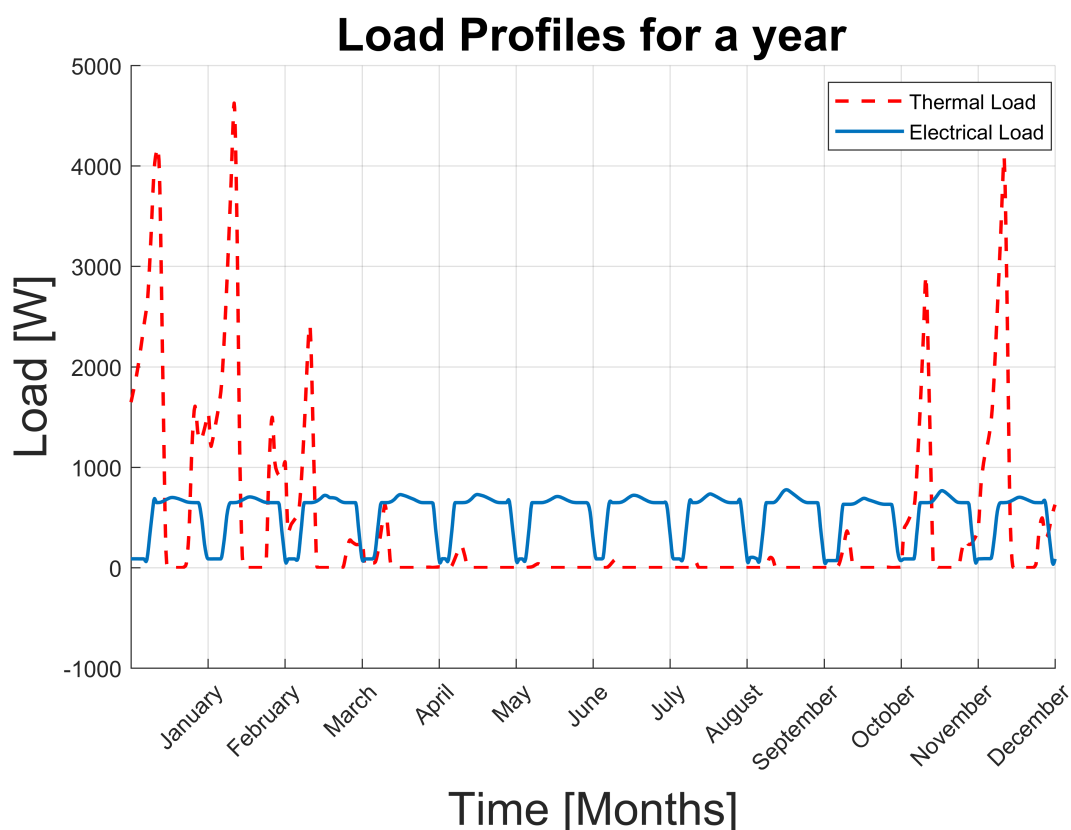


**Figure 6.1:** Load demanded by the greenhouse for the whole year for the location in Jeddah, Saudi Arabia. The red dashed line represents the thermal load [W] and the blue line represents the electric load [W] of the greenhouse.

In figure 6.1, the load required by the greenhouse for the whole year is represented. The thermal load is high for the months of December, January and February with the maximum thermal load reaching about 4500 W. During the summer, as the ambient temperature is high, the requirement of thermal load is not present. Therefore, during the summer months, the thermal load is mostly zero.

Figure 6.2 shows the normalised mass flow and temperature through the solar field for a day in winter. On the right-hand y axis of the figure 6.2 the irradiation is represented in  $\text{W}/\text{m}^2$ . As can be seen, during winter, the maximum irradiation incident of the flat plate solar collectors reaches  $700 \text{ W}/\text{m}^2$  approximately. The irradiation is maximum around noon which is as expected.

The temperature at the inlet of the solar field is represented by TT001 and the temperature at the exit of the solar field is given by TT002. As defined by the control, it is ideal for the temperature at the outlet of the SF should be set at  $90^\circ\text{C}$ . It can be

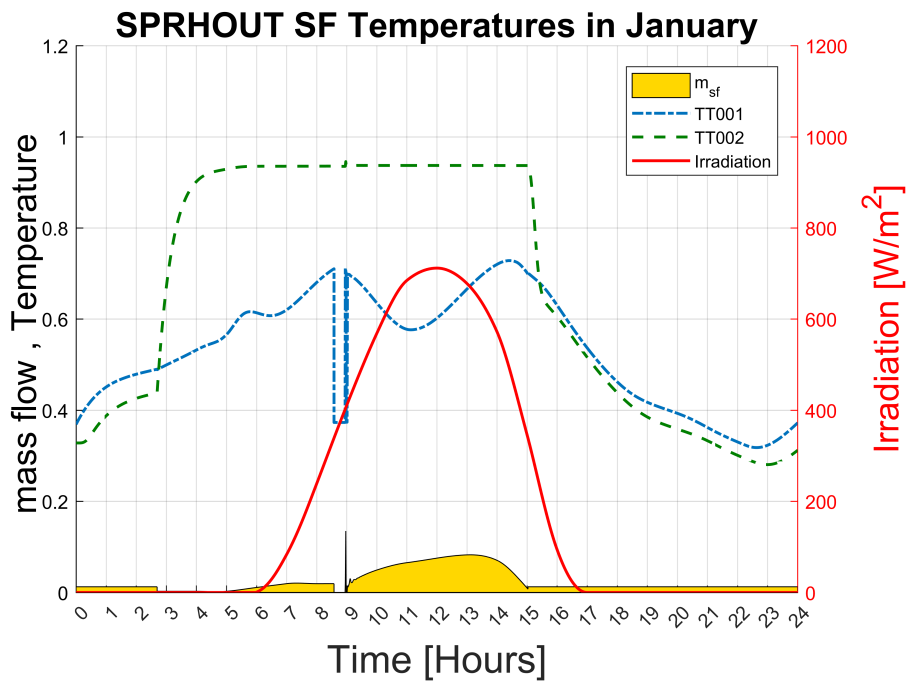
seen that during the early hours of the day, since the irradiation incident on the solar field is below the threshold irradiation of  $340 \text{ W/m}^2$  defined by the control logic, the SF is in an OFF state during that time. As the energy in the TES, initially, is below the minimum required by the ORC power unit, therefore the gas burner is turned on. This can be seen when the temperature TT002 starts to rise until it reaches the optimum temperature of  $90^\circ\text{C}$ .

The mass flow through the SF initially is very low as the SF is turned off. Since in the simulation software, using a value of zero for mass flow is not permitted, therefore we see a very low value of the mass flow signifying that the contribution of the SF towards the energy in the TES is negligible.

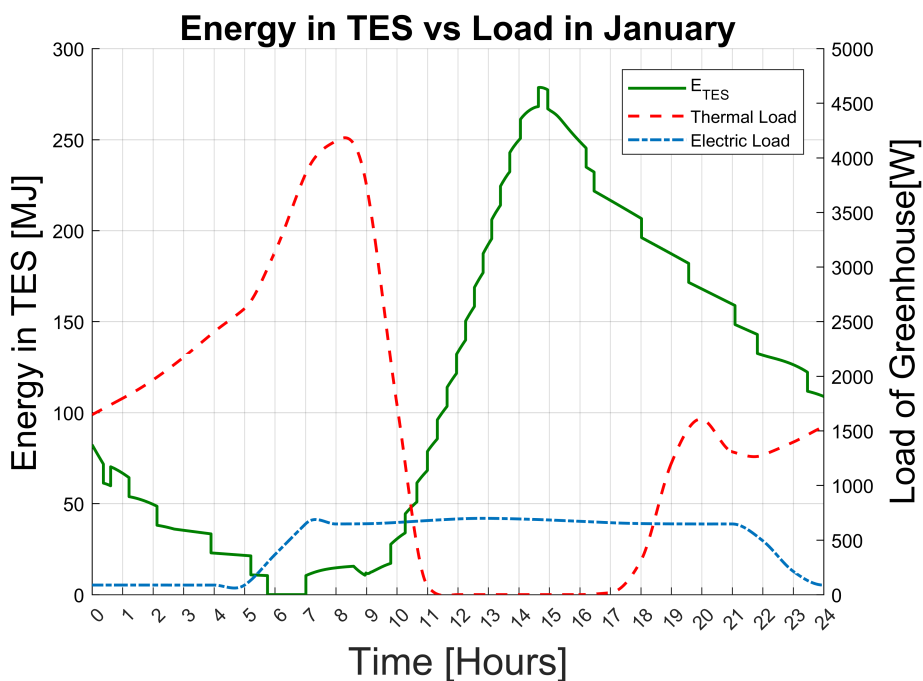
If we focus on the TT001, the sudden drop in temperature around 8 am in the day is observed as the gas burner is turned OFF and the SF is turned ON as the irradiation incident on the solar field rises above the threshold limit. This allows the mass flow through the solar field to be controlled by the PI controller through the pump P001. During this time, the thermal energy storage is also charged up. As the day progresses, the irradiation levels drop below the threshold again and the solar field is switched OFF.

Now since there is enough energy in the thermal energy storage, the gas burner remains in an OFF state and the TES is discharged. Thus we see a drop in temperature TT002 from the set limit of  $90^\circ\text{C}$ .

Figure 6.3 displays the energy in the thermal energy storage with respect to the electrical and thermal loads of the greenhouse. As discussed earlier, during the initial hours of the day as the irradiation received by the solar field is below the threshold irradiation, the SF remains in an OFF state. Thus, the TES gets discharged until the gas burner is switched on, which can be observed from the figure 6.3.



**Figure 6.2:** Dynamic simulation results of the SPRHOUT model during a reference winter day in Jeddah, Saudi Arabia. Temperature sensors TT001 and TT002 represents the normalised inlet and outlet temperatures of the solar field.  $m_{SF}$  represents the mass flow through the solar field and the red line represents the Irradiation.



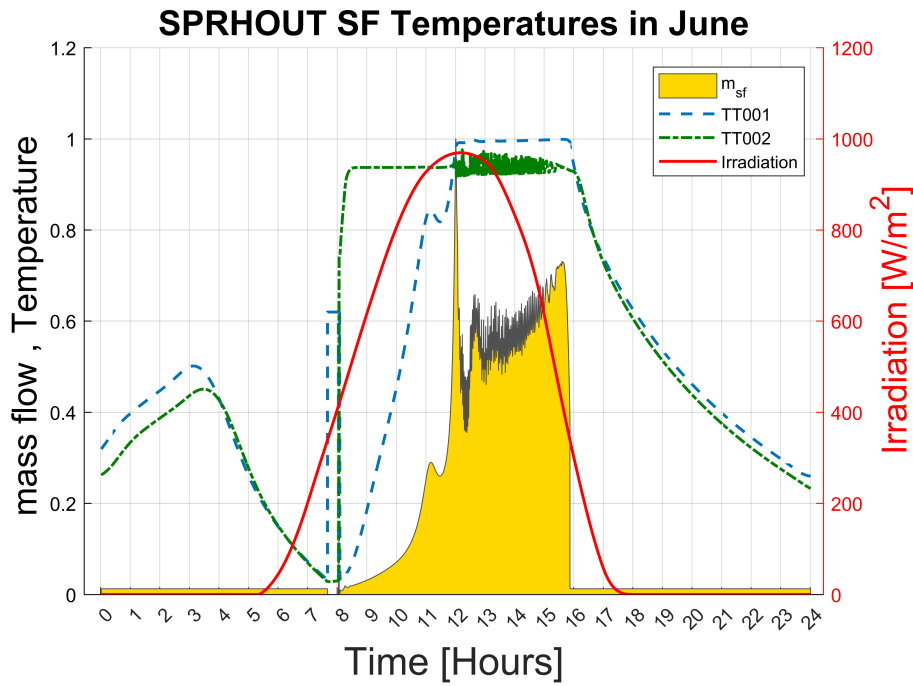
**Figure 6.3:** Dynamic simulation results of the SPRHOUT model during a reference winter day in Jeddah, Saudi Arabia. The left y axis represents the energy in TES given in MJ. The right y-axis represents the thermal and electrical loads in W.

Figure 6.4 shows the simulation result for the mass flow through the solar field along with the inlet and outlet temperatures of the solar field for a day in summer. The irradiation received by the flat plate collectors is plotted on the right y-axis. As expected, the irradiation received in the summer is approximately  $1000 \text{ W/m}^2$  which is higher in comparison to the winter season.

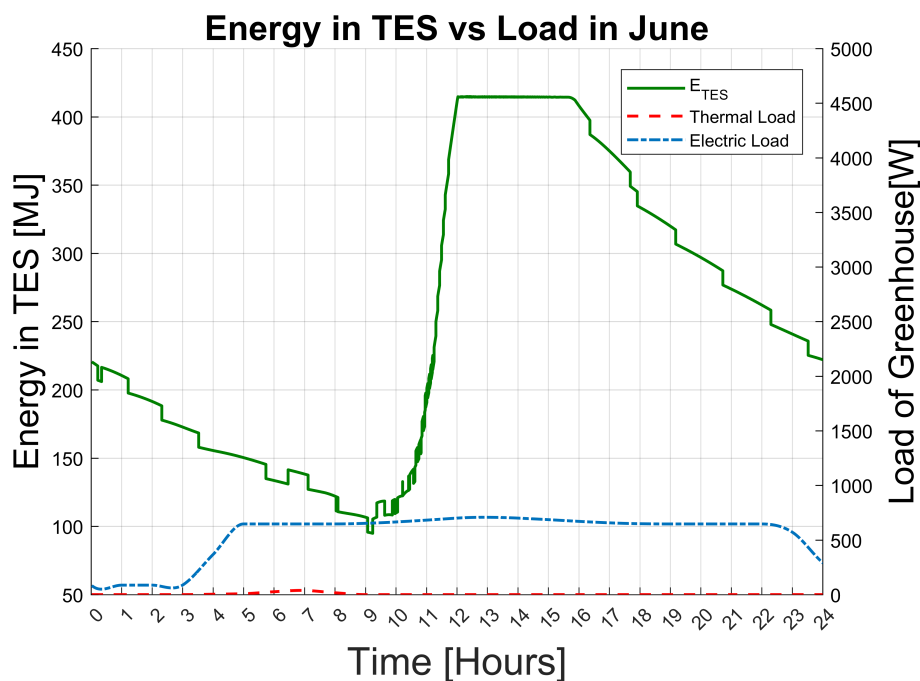
It should be noted that the heating requirement for the greenhouse is almost negligible during the summer period as compared to the heating required during winter. During the summer, the main requirement for the greenhouse is the electrical load shown by the figure 6.5.

At the start of the day, the solar field is in an OFF state due to the irradiation being below the threshold irradiation. During that time, the TES gets discharged which can be seen in figure 6.5. As there is enough energy in the TES to run the ORC power unit, the gas burner is in an OFF state as it is not required. As soon as the irradiation incident on the flat plate collectors crosses the threshold, the solar field switches ON and the mass flow through the solar field is then controlled by the PI controller. Figure 6.4 shows the increase in temperature at the exit of the solar field TT002 to the optimum level set at  $90^\circ\text{C}$ . It should be noted that the rise in temperature TT001 occurs during the day due to the fact that it is a closed loop system and as the TES gets full, the inlet temperature through the SF also increases. This is validated by the constant energy in TES seen in figure 6.5 around 12 pm where the TES is fully charged.

As the day goes on, the irradiation level drops and the solar field is turned OFF when the irradiation drops below the threshold level. As the TES is fully charged during that point, it can provide the energy to run the ORC plant without the need to use the gas burner. During summer, the use of gas burner is zero due to enough energy being provided by the TES to meet the electrical load requirements of the greenhouse.



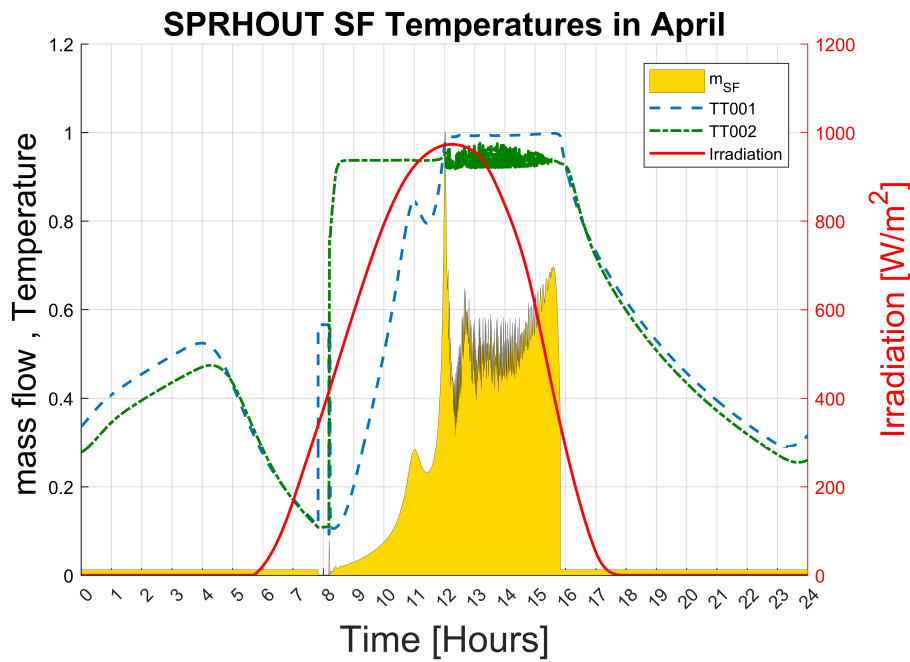
**Figure 6.4:** Dynamic simulation results of the SPRHOUT model during a reference summer day in Jeddah, Saudi Arabia. Temperature sensors TT001 and TT002 represents the normalised inlet and outlet temperatures of the solar field.  $m_{SF}$  represents the mass flow through the solar field. On the right y-axis, the irradiation incident on the solar field is plotted.



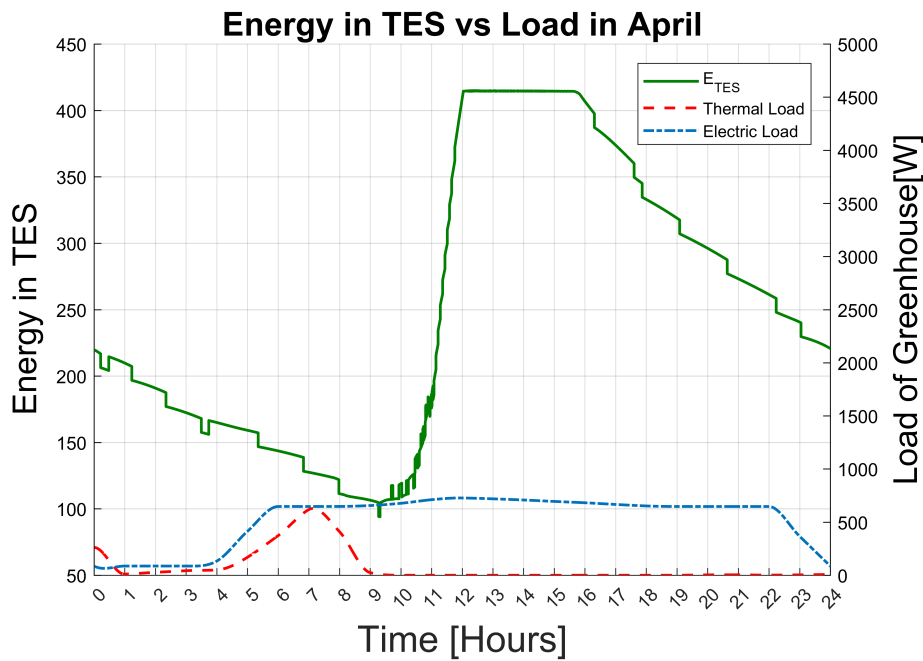
**Figure 6.5:** Dynamic simulation results of the SPRHOUT model during a reference summer day in Jeddah, Saudi Arabia. The left y axis represents the energy in TES given in MJ. The right y-axis represents the thermal and electrical loads in W.

Figure 6.6 shows the results from the simulation for a day in April. Looking closely, it can be seen that performance of the SPRHOUT system is similar to the previous days in the summer and winter. The fluctuations observed, for the temperature TT002, are due to the PI controller changing the input to the pump P001 in order to maintain the temperature at the outlet of the solar field at 90°C.

Again, looking at the load for the greenhouse during spring, it is seen that the dominating factor is the electrical load reaching approximately 100 W. The thermal load is mostly negligible and is only present for a small duration during the day. The energy in TES is thus sufficient to satisfy the load demands of the greenhouse. Around 12pm, the TES reaches its maximum limit after which it remains at that limit and finally starts to discharge when the solar field is switch OFF.



**Figure 6.6:** Dynamic simulation results of the SPRHOUT model during a reference spring day in Jeddah, Saudi Arabia. Temperature sensors TT001 and TT002 represents the normalised inlet and outlet temperatures of the solar field.  $m_{SF}$  represents the mass flow through the solar field. On the right y-axis, the irradiation incident on the solar field is plotted.



**Figure 6.7:** Dynamic simulation results of the SPRHOUT model during a reference spring day in Jeddah, Saudi Arabia. The left y axis represents the energy in TES given in MJ. The right y-axis represents the thermal and electrical loads in W.

Similar simulation results for the month of October are presented in figures 6.8 and 6.9. The mass flow and temperatures at the inlet and exit of the solar field are normalised and plotted with respect to the irradiation incident of the solar field.

During the Autumn season, the TES has enough energy to match the load requirements of the greenhouse. The maximum thermal load required in the October can be observed to be approximately 80 W and the electrical load is almost constant at 100 W.

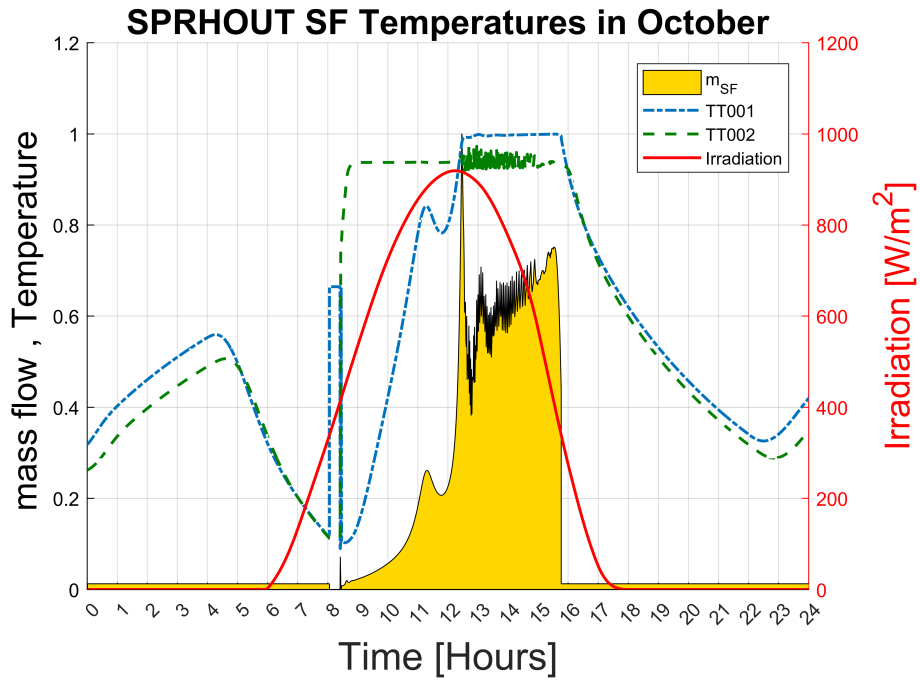


**Figure 6.8:** Dynamic simulation results of the SPRHOUT model during a reference autumn day in Jeddah, Saudi Arabia. Temperature sensors TT001 and TT002 represents the normalised inlet and outlet temperatures of the solar field.  $m_{SF}$  represents the mass flow through the solar field. On the right y-axis, the irradiation incident on the solar field is plotted.

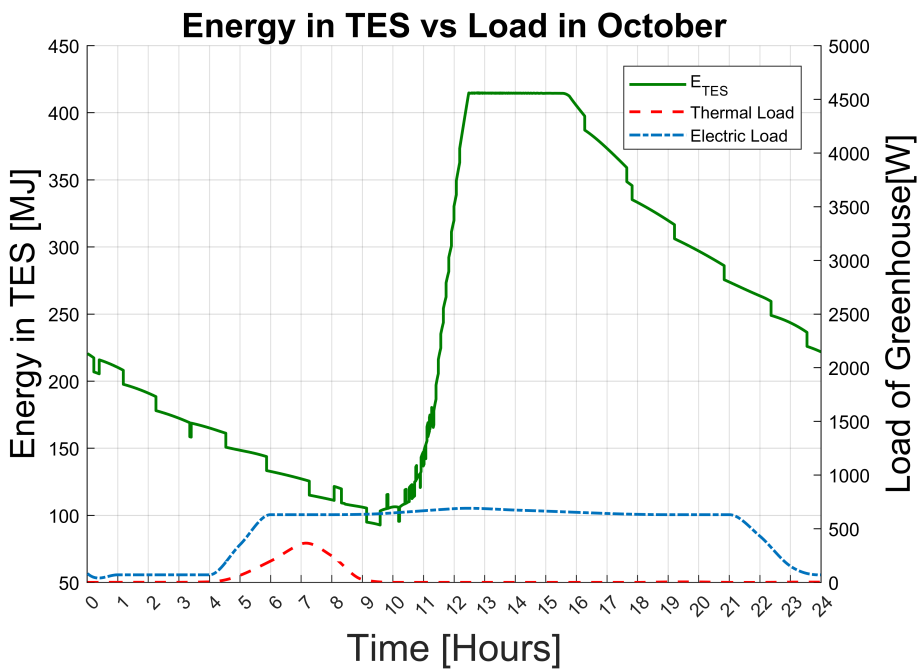


**Figure 6.9:** Dynamic simulation results of the SPRHOUT model during a reference autumn day in Jeddah, Saudi Arabia. The left y axis represents the energy in TES given in MJ. The right y-axis represents the thermal and electrical loads in W.

### 6.3. SPRHOUT economic analysis

In order to investigate the effect of the selected control strategy on the economic profitability of the SPRHOUT system, an annual analysis was performed using the developed dynamic model. Two economic investigations are performed: one considering only the SPRHOUT system and the other one considering the SPRHOUT coupled to the greenhouse.

The first comparison performed was considering only the SPRHOUT system. In order to calculate the NPV, the CAPEX and OPEX of the SPRHOUT system had to be calculated. The CAPEX, which is the capital expenditure, depends on the sizing of the SPRHOUT system which influences the investment required by the plant. Thus, the sizing of the solar field, the TES unit and the power unit plays an important factor in this regard. The sizing of the solar field is of particular importance as it provides the thermal energy required to match the thermal and electrical load demands of the greenhouse.

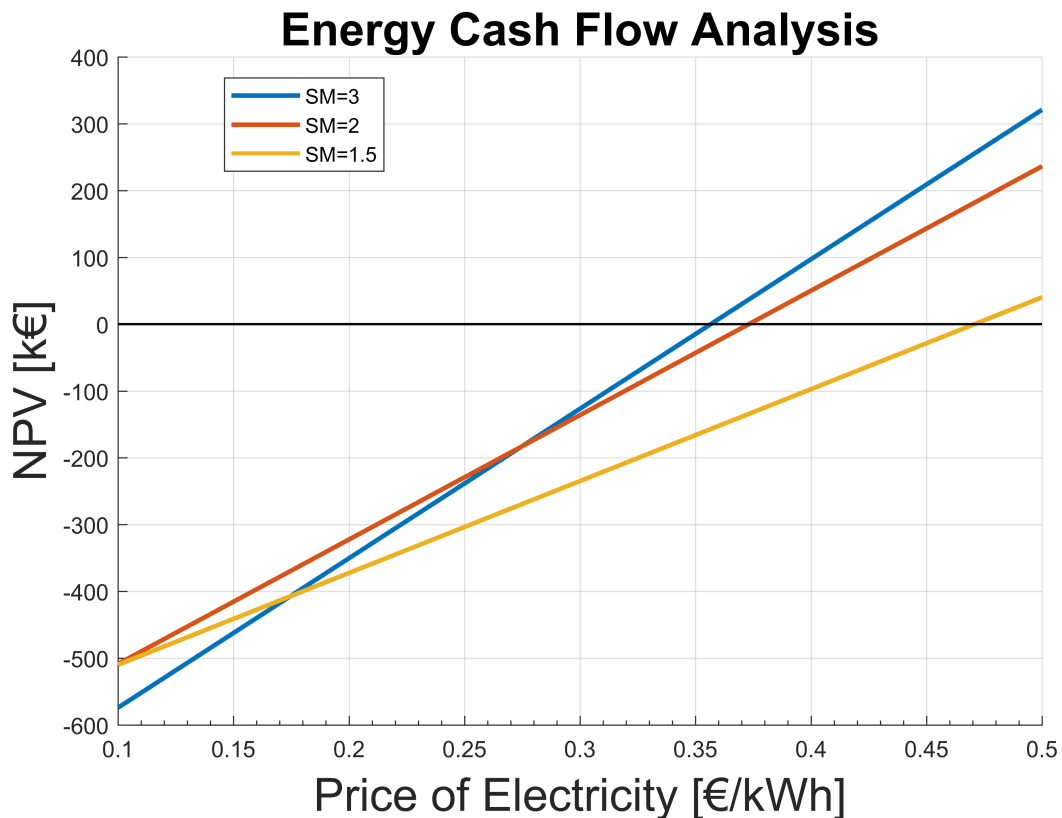


**Figure 6.10:** Energy cash flow analysis. The figure shows the NPV vs the electricity price for different sizing of the solar field using the solar multiple factor. Figure represents SM=1.5,2,3 for which the NPV is calculated.

The solar multiple (SM) is a parameter which would influence the Net Present Value and Payback time of the SPRHOUT system. The Net present value was calculated for the SPRHOUT system for different prices of electricity and using different solar multiple values to see how the sizing of the solar field affects the NPV of the system along with the price of electricity. Figure 6.10 represents the NPV calculated for the

SPRHOUT system versus the changing price of electricity given in €/kWh. It can be seen that for a SM value of 3, the price of electricity required to achieve a positive NPV is approximately around €0.36/kWh. The price of electricity, for which the NPV for the system becomes positive, increases with the decrease in the solar multiple value. Simulation performed for SM=1.5 shows that the price of electricity is higher in comparison to SM=3 at around €0.47/kWh approximately. It can be concluded that as the size of the solar field increases, the selling price of electricity is lower in order for the NPV to achieve a positive value, thus making the project economically viable.

In the case when the SPRHOUT and the greenhouse are considered together, the price of selling the tomatoes is assumed to be €2/kg with a specific yield of 85 Kg/m<sup>2</sup>/yr. The NPV and payback time for different solar multiples are summarised in table 6.5.

<b>Parameter</b>	<b>SM = 1.5</b>	<b>SM = 2</b>	<b>SM = 3</b>
<b>CAPEX [kEuros]</b>	628.42	684.81	798.91
<b>OPEX [kEuros]</b>	26.954	19.14	12.74
<b>NPV [kEuros]</b>	7675.83	7701.51	7654.69
<b>PBT [Years]</b>	4.580	4.554	4.472

**Table 6.5:** Economic Parameters for a SPRHOUT plant in Jeddah, Saudi Arabia. CAPEX represents the capital expenditure and the OPEX represents the operating expenditure of the whole plant including SPRHOUT and greenhouse.

From the table 6.5, it is clear that for different sizing of the solar field, the NPV and the PBT changes. The NPV is highest for a solar multiple of 2 having a value of k€7701.51. For a higher solar multiple value, even though the field operating cost of the field is the lowest, the capital expenditure increases which influences the NPV value. For a smaller SM value of 1.5, the capital expenditure is the lowest. But this implies that the energy provided by the solar field might not be enough thus requiring burning more fuel using the gas burner to provide heat to match the thermal load requirements of the greenhouse. Hence, the operating cost for SM=1.5 is the highest. This results in the NPV being affected. The optimum value for the SM is found to be 2 where the NPV is the highest along with the lowest payback time, which is advantageous to the owner of the greenhouse. Figure 6.11 represents the optimum value for the solar field size where the NPV is maximum.

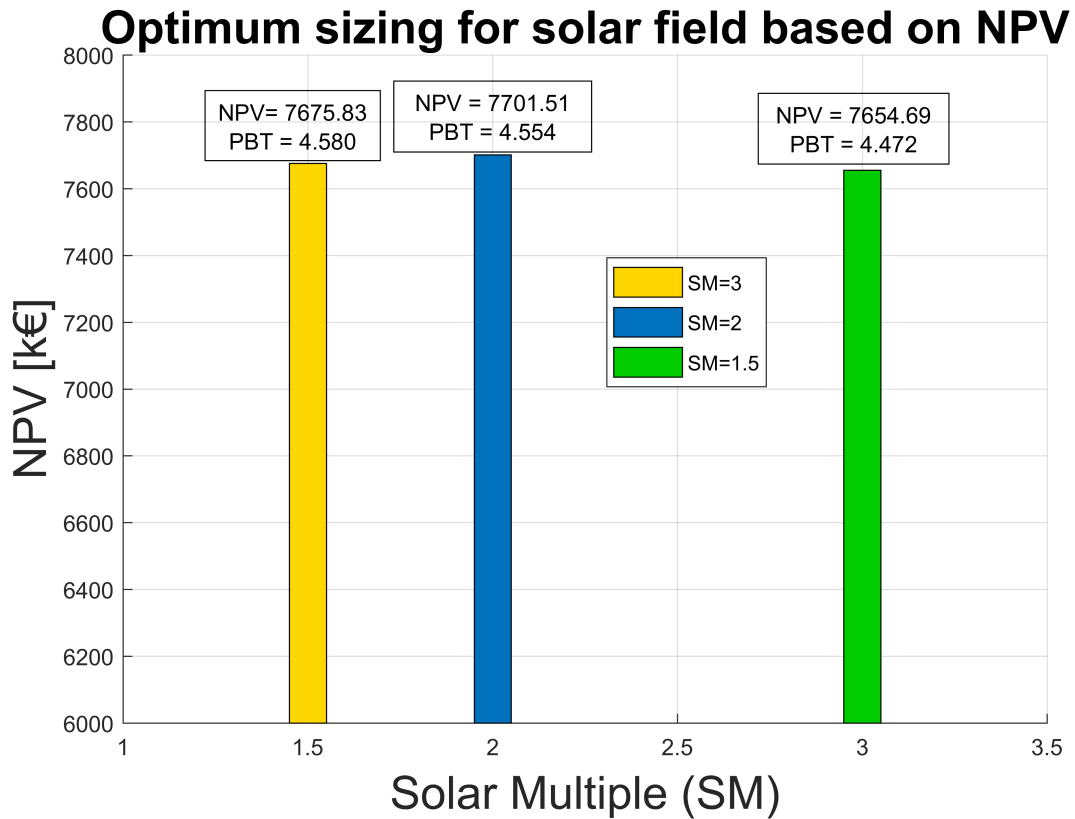


**Figure 6.11:** Optimum sizing of the solar field based on NPV. The configuration of SM=2 results in maximum NPV for the project in Jeddah, Saudi Arabia, thus representing the optimum sizing for the solar field.

A similar comparison was performed for the NPV of SPRHOUT with variable gas prices. Figure 6.12 represents the gas prices versus the NPV of the SPRHOUT system (only considering the energy cash flow). As discussed previously, the analysis was performed for different sizes of the solar field using different values of the solar multiple.

In the figure 6.12, the gas prices are represented in €/Nm<sup>3</sup>, where Nm<sup>3</sup> is the normalised cubic metre value for the amount of gas used. It can be seen that for different solar multiples, the gas price has to be quite high for the NPV to achieve a positive value. Taking the example of SM=3, the price of gas is approximately around €2.6/Nm<sup>3</sup> for the project to be economically feasible.

As can be seen from the result, the price of the gas is quite high for the project to be economically feasible. This isn't an ideal case for a real life project. The value of the gas prices will change however when certain incentives such as the carbon tax are included which would promote the use of renewable energy sources. Most of the countries in the world impose a carbon tax based on the amount of CO<sub>2</sub> burnt. The rate of the carbon tax varies from country to country.

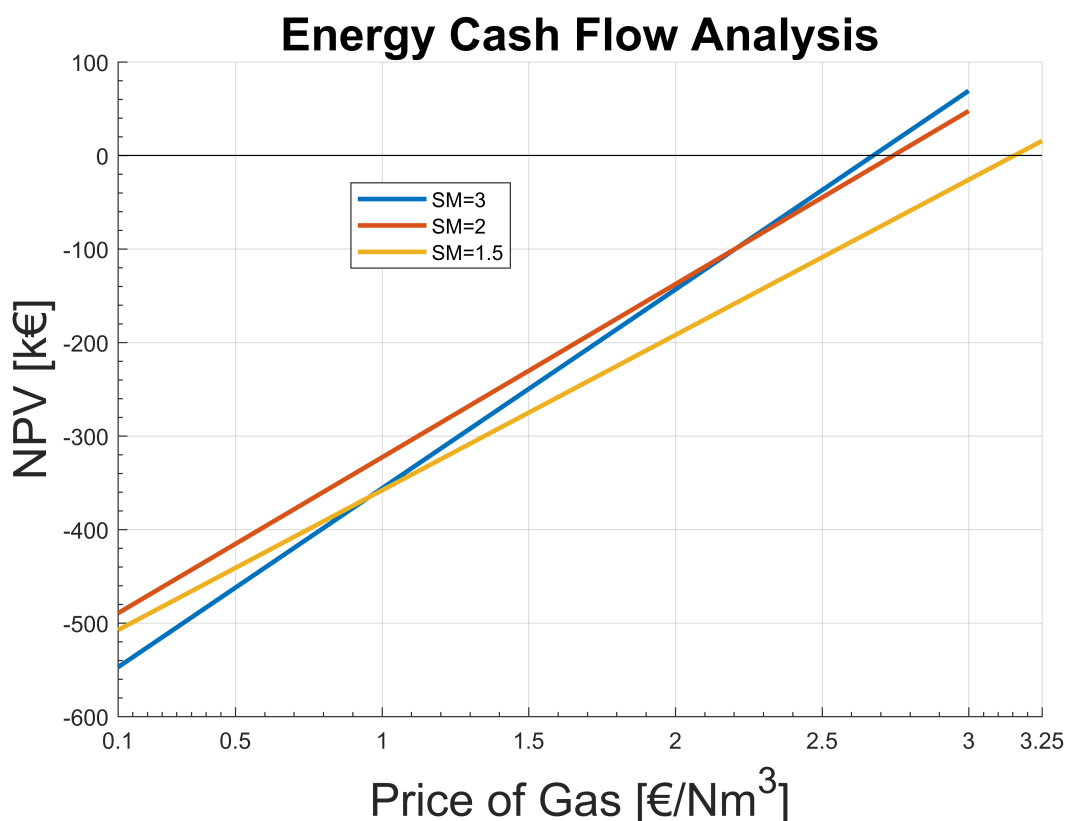


**Figure 6.12:** Energy cash flow analysis. The figure shows the NPV vs the gas price for different sizing of the solar field using the solar multiple factor. Figure represents SM=1.5,2,3 for which the NPV is calculated.

In our case, a carbon tax rate of € 120/metric ton of CO<sub>2</sub> is used [26]. This is an optimistic scenario though having a lot of relevance as the world moves towards a green economy. Using this value, the previous analysis was repeated and the result shown in figure 6.13. According to the figure 6.13, the price of gas for which the NPV becomes positive is lower as compared to the scenario where no carbon tax is implemented. For SM=3, the gas price is approximately € 1.3/Nm<sup>3</sup>, which is lower in comparison with the previous case where carbon tax was not implemented.

As the society in the future adopts a more aggressive strategy by implementing higher carbon tax rates, the project will become more economically viable as compared to just using a gas burner for providing thermal heat.

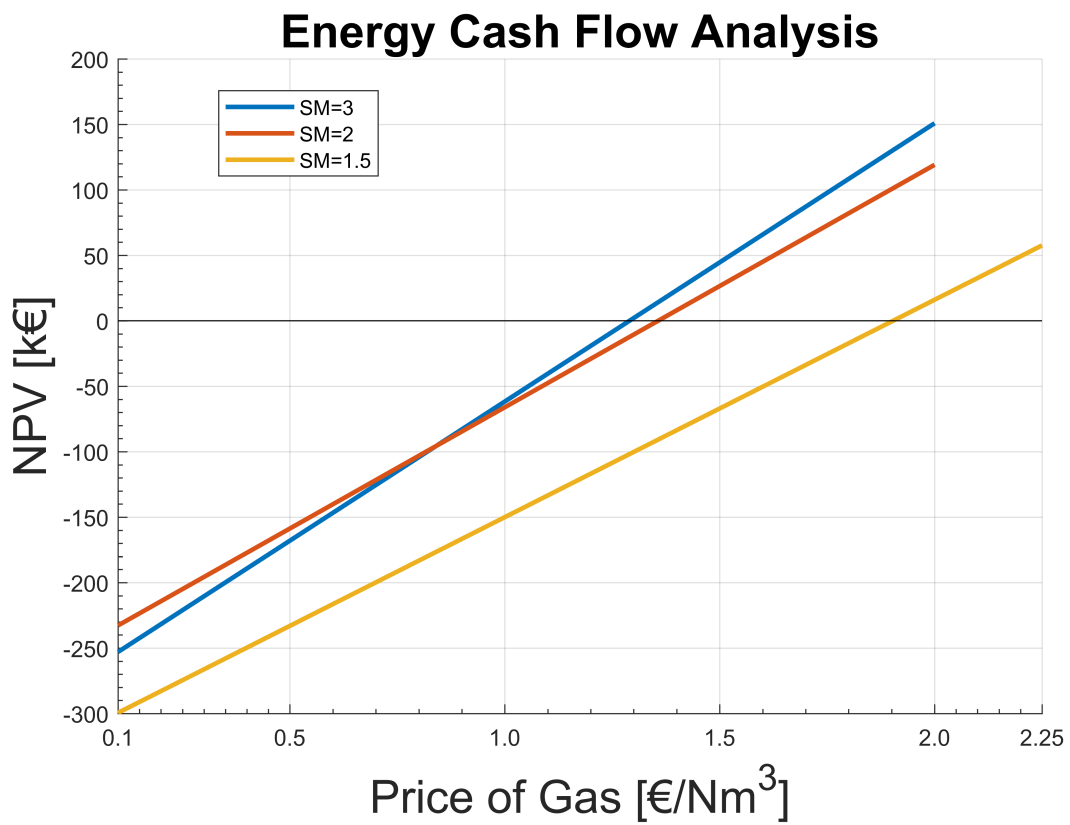


**Figure 6.13:** Energy cash flow analysis but with carbon tax implemented. The figure shows the NPV vs the gas price for different sizing of the solar field using the solar multiple factor. Figure represents SM=1.5,2,3 for which the NPV is calculated.

# 7

## Conclusions

In this thesis, the original results related to the steady-state and dynamic modelling of the Solar Powered Horticultural Off-Grid UniT (SPRHOUT) developed by SOLHO are outlined. The thesis is based on 6 main chapters. The main outcomes of each chapter are summarised below:

The first chapter introduces the energy scenario of the horticulture industry and presents the current technologies in use in the horticulture sector. The framework for the thesis is defined and the main research questions are formulated.

The second chapter introduces the SPRHOUT (Solar PowerRed Horticulture Off-grid UniT) technology developed by SOLHO which provides energy to the greenhouse using solar thermal collectors and thermal energy storage. A techno-economic case study is performed for a location in Greece, where the SPRHOUT system is compared with a system consisting of PV+gas burner. The preliminary analysis shows that the CAPEX and OPEX of SPRHOUT for a 5 Ha greenhouse is lower as compared to PV + gas burner system mostly due to the cost of batteries. It is important to note that this result is dependent on the location chosen and may vary depending on the cost of gas and reliability of the electric grid.

The third chapter gives an introduction on dynamic modelling and introduces the Modelica language. The open source ThermoCycle library is described with the main models used in the thesis are discussed. This lays the foundation for the SPRHOUT Modelica library.

Chapter 4 discusses the SPRHOUT Modelica model and describes the different components used in the model: the flat plate collector, the Thermal Energy Storage (TES), the organic Rankine cycle (ORC) power block, the expansion tank, the gas burner, the PI (Proportional-Integral) control block and the fan. Finally, an overview of the whole SPRHOUT system is presented.

Chapter 5 describes the different control strategies used for the simulation of SPRHOUT. The initial control strategy is discussed where the temperature at the outlet of the solar field is considered as the main control parameter. The energy level inside the TES was not accounted for in this strategy which prompted the design of a new control

strategy. The final control strategy was presented which took into account the energy levels inside the TES and controlled the switching of the SF and the gas burner according to the requirement. This strategy was analysed in detail in the results chapter.

Chapter 6 reports the results obtained from the SPRHOUT model simulation. The model was run to investigate the control logic on a daily basis and the control strategies on an annual basis.

- For the control logic analysis, an electrical load of  $1 \text{ kW}_{el}$  was considered and the different input parameters for all the components used in the SPRHOUT were described. Similarly, the initial parameters for the economic analysis were described. The concept of Net Present Value (NPV) and the Payback time (PBT) was explained in detail. Section 6.2 discussed the control logic simulation where the results from the dynamic SPRHOUT Modelica model was presented for one day of each season, i.e., winter, summer, spring and autumn. It was seen that the use of gas burner was limited to a short period in winter. During the rest of the year, the SPRHOUT performed as per the control logic formulated in chapter 5.
- For the economic analysis, a case study was defined for a greenhouse facility with an electric load of  $50 \text{ kW}_{el}$ . The SPRHOUT system was scaled up to match the electrical load and the simulation was performed for the year. The parametric analysis of NPV vs the electric grid was presented for different solar multiples (SM=1.5, 2, 3) for the SPRHOUT system only and then for the SPRHOUT coupled with the greenhouse. It can be concluded that as the size of the solar field increases, the selling price of electricity is lower in order for the NPV to achieve a positive value, thus making the project economically viable. This value significantly decreases when the NPV for SPRHOUT coupled with the greenhouse is calculated (due to the inclusion of revenue from selling of the crop). The optimum size is achieved in such a case for a SM of 2.
- • The final analysis is performed where the NPV of the SPRHOUT system is compared with the gas price. It is seen that for different solar multiples, the price of gas required to make the project economically feasible is high with a value of  $\text{€ } 2.6/\text{Nm}^3$ . Thus, a need for incentives emerged. When the carbon tax was introduced, it was seen that the gas prices becomes lower in such a case, thus presenting a case where the project can become economically viable.

## 7.1. Recommendations for future work

The developed dynamic model of the SPRHOUT performs effectively in the daily simulations as shown in chapter 6. In light of the obtained results, further work needs to be performed in order to validate the dynamic model with experimental results. Furthermore, it was proven that the modelling approaches adopted in the SPRHOUT library led to satisfactory results for the simulation of small capacity thermal systems. Further developments should focus on implementing models capable of handling the simulation of cold start-up or shut-down conditions, i.e. zero flow rate in the tubes.

Furthermore, the annual simulation of the presented model was based on a 12 days simulation where each day was representative of a month in the year in order to reduce the computational time. The development of the model for large systems that simulates the hourly data on an annual basis is seen as the next step. The data obtained from the model would provide an even more accurate representation in terms of the performance of the SPRHOUT.



# Bibliography

- [1] United Nations DESA. Probabilistic projections of world population. <https://population.un.org/wpp/Graphs/Probabilistic/POP/TOT/>, 2017.
- [2] UNFCCC. The paris agreement. <https://unfccc.int/process-and-meetings/the-paris-agreement/the-paris-agreement>, 2018.
- [3] EIA. Internation energy outlook 2018. <https://www.eia.gov/outlooks/ieo/>, 2018.
- [4] Sunbelt countries could have 1.1 tw solar pv by 2030. <http://www.renewableenergyfocus.com/view/13547/sunbelt-countries-could-have-1-1-tw-solar-pv-by-2030/>, October 2010.
- [5] Climate impacts on agriculture and food supply. [https://19january2017snapshot.epa.gov/climate-impacts/climate-impacts-agriculture-and-food-supply\\_.html](https://19january2017snapshot.epa.gov/climate-impacts/climate-impacts-agriculture-and-food-supply_.html), October 2016.
- [6] Netherlands-worlds biggest exporter. <https://www.freshplaza.com/article/2135083/netherlands-world-s-biggest-re-exporter-for-11-fruit-veg-products/>, 2015.
- [7] Wageningen University and Research. Energy scenario in the dutch horticulture industry. [https://www.wur.nl/upload\\_mm/1/d/8/7b39207c-8eed-442d-80cc-1c7f1cbba8b9\\_WUR\\_TuinbouwCO2emissie\\_Print\\_A4\\_ENG.PDF](https://www.wur.nl/upload_mm/1/d/8/7b39207c-8eed-442d-80cc-1c7f1cbba8b9_WUR_TuinbouwCO2emissie_Print_A4_ENG.PDF), October 2016.
- [8] Netherlands: Greenhouse vegetable area vs. number of farms. <https://www.hortidaily.com/article/6040981/netherlands-greenhouse-vegetable-area-vs-number-of-farms/>, September 2018.
- [9] LEI Wageningen UR. The power of dutch greenhouse vegetable horticulture. <http://edepot.wur.nl/27928>, August 2008.
- [10] FAO. Save and grow. <http://www.fao.org/ag/save-and-grow/en/index.html>.
- [11] Sundropfarms. Sundrop system. <http://www.sundropfarms.com/sundrop-system/>.

- [12] Hortidaily. Switzerland: Pumps restarted for geothermal heating of greenhouses. <https://www.hortidaily.com/article/6044144/switzerland-pumps-restarted-for-geothermal-heating-of-greenhouses/>, June 2018.
- [13] UNU-GTP and LaGeo. Geothermal energy in horticulture. <https://orkustofnun.is/gogn/unu-gtp-sc/UNU-GTP-SC-18-23.pdf>, March 2014.
- [14] DAGO. Master plan geothermal energy in the netherlands. [https://geothermie.nl/images/bestanden/Masterplan\\_Aardwarmte\\_in\\_Nederland\\_ENG.pdf](https://geothermie.nl/images/bestanden/Masterplan_Aardwarmte_in_Nederland_ENG.pdf), May 2018.
- [15] DAGO. Geothermal energy. <https://www.dago.nu/en/geothermal>, 2019.
- [16] Get.Invest. Renewable energy potential in kenya. <https://www.get-invest.eu/market-information/kenya/renewable-energy-potential/>.
- [17] Green Farming. Cost-effective use of solar energy in east african horticulture. [https://www.solarthermalworld.org/sites/default/files/story/2015-03-03/green\\_farming\\_kenya\\_solar\\_brochure\\_2.pdf](https://www.solarthermalworld.org/sites/default/files/story/2015-03-03/green_farming_kenya_solar_brochure_2.pdf), October 2013.
- [18] Powering Agriculture. Sunchill: Solar cooling for horticultural preservation. <https://poweringag.org/innovators/sunchill-solar-cooling-horticultural-preservation>.
- [19] P.Colonna E. Casati, A. Galli. Thermal energy storage for solar-powered organic rankine cycle engines. <https://doi.org/10.1016/j.solener.2013.07.013>, October 2013.
- [20] E. Rojas R. Bayon. Simulation of thermocline storage for solar thermal power plants: From dimensionless results to prototypes and real-size tanks. <https://doi.org/10.1016/j.ijheatmasstransfer.2013.01.047>, February 2013.
- [21] A. Desideri et al. Steady-state and dynamic validation of a small-scale waste heat recovery system using the thermocycle modelica library. <https://doi.org/10.1016/j.ijheatmasstransfer.2013.01.047>, September 2016.
- [22] A. Desideri et al E. Casati. Preliminary assessment of a novel small csp plant based on linear collectors, orc and direct thermal storage. <https://orbi.uliege.be/bitstream/2268/205799/1/Paper.pdf>, January 2012.
- [23] A. Desideri. Dynamic modeling of organic rankine cycle power systems. , 2016.
- [24] European Commission. Tmy generator. <https://re.jrc.ec.europa.eu/pvgis5/tmy.html>.

- 
- [25] GREENoneTECH. Gk 3003 series single and double glazed large-size collectors. [https://aalborgcsp.com/fileadmin/user\\_upload/beUId/1/1-Downloadable\\_materials/1-Brochures/2015-10-28\\_Aalborg\\_CSP\\_GREENoneTEC\\_flat\\_panel\\_datasheet\\_2-pager\\_ENG.pdf](https://aalborgcsp.com/fileadmin/user_upload/beUId/1/1-Downloadable_materials/1-Brochures/2015-10-28_Aalborg_CSP_GREENoneTEC_flat_panel_datasheet_2-pager_ENG.pdf).
- [26] Carbon Tax Center. Where carbon is taxed. <https://www.carbontax.org/where-carbon-is-taxed/>.